

Prenatal environment is associated with the pace of cortical network development over the first three years of life

Received: 14 August 2023

Accepted: 30 August 2024

Published online: 11 September 2024

 Check for updates

Ursula A. Tooley¹✉, Aidan Latham², Jeanette K. Kenley², Dimitrios Alexopoulos², Tara A. Smyser¹, Ashley N. Nielsen², Lisa Gorham¹, Barbara B. Warner³, Joshua S. Shimony⁴, Jeffrey J. Neil^{2,4}, Joan L. Luby², Deanna M. Barch^{1,4,5}, Cynthia E. Rogers^{1,3} & Christopher D. Smyser^{1,2,3,4}

Environmental influences on brain structure and function during early development have been well-characterized, but whether early environments are associated with the pace of brain development is not clear. In pre-registered analyses, we use flexible non-linear models to test the theory that prenatal disadvantage is associated with differences in trajectories of intrinsic brain network development from birth to three years ($n = 261$). Prenatal disadvantage was assessed using a latent factor of socioeconomic disadvantage that included measures of mother's income-to-needs ratio, educational attainment, area deprivation index, insurance status, and nutrition. We find that prenatal disadvantage is associated with developmental increases in cortical network segregation, with neonates and toddlers with greater exposure to prenatal disadvantage showing a steeper increase in cortical network segregation with age, consistent with accelerated network development. Associations between prenatal disadvantage and cortical network segregation occur at the local scale and conform to a sensorimotor-association hierarchy of cortical organization. Disadvantage-associated differences in cortical network segregation are associated with language abilities at two years, such that lower segregation is associated with improved language abilities. These results shed light on associations between the early environment and trajectories of cortical development.

The first years of life are a time of rapid brain development, with intrinsic cortical organization becoming refined and large-scale brain systems developing into their adultlike configuration^{1,2}. As children mature, intrinsic cortical networks become more segregated^{3,4}, with sets of brain regions displaying more densely interconnected patterns of connectivity and large-scale systems becoming increasingly distinct^{2,5-7}. This refinement of cortical organization occurs in a spatiotemporally patterned manner, with maturation occurring earlier in

primary sensory regions than transmodal association regions⁸. The development of cortical network segregation also has implications for cognition, with higher levels of cortical network segregation associated with better cognitive abilities in adolescents and adults^{6,9-12}. One environmental factor that is associated with the development of cortical network segregation – as well as many later life outcomes, including physical wellbeing^{13,14}, cognitive ability¹⁵, and mental health¹⁶ – is disadvantage. Disadvantage is a broad and multifaceted construct

¹Department of Psychiatry, Washington University in St. Louis, St. Louis, MO, USA. ²Department of Neurology, Washington University in St. Louis, St. Louis, MO, USA. ³Department of Pediatrics, Washington University in St. Louis, St. Louis, MO, USA. ⁴Department of Radiology, Washington University in St. Louis, St. Louis, MO, USA. ⁵Department of Psychological and Brain Sciences, Washington University in St. Louis, St. Louis, MO, USA. ✉e-mail: tooley@wustl.edu

that encompasses measures of socioeconomic status (SES) such as income, education, and occupational prestige^{17,18}, as well as related health factors such as insurance and diet quality¹⁹.

Relations between disadvantage and the development of cortical network segregation have been predominantly examined in older children and adolescents. In youth ages 8–22 years, SES moderated age-associated increases in cortical network segregation, such that youth from more economically advantaged backgrounds started with lower cortical network segregation but showed a steeper increase in cortical network segregation during adolescence than youth from less economically advantaged backgrounds, thus ending with higher levels of cortical network segregation at 22 years²⁰. Associations between SES and cortical network segregation were also found in youth ages 6–17 years living in low-SES neighborhoods²¹. Collectively, these studies suggest that disadvantage may accelerate the pace of cortical network segregation earlier in development, setting the stage for associations observed in older children and adolescents²². More broadly, associations between disadvantage and intrinsic brain organization are visible as early as the first month of life^{23,24}, but as of yet no longitudinal studies have examined how disadvantage relates to the development of cortical network segregation during the critical first years of life.

The pace of early brain development has been associated with important risk factors and behavioral outcomes. Changes in the pace of brain development have been linked to psychiatric disorders^{25–27}, and accelerated pubertal development is associated with poorer mental health during adolescence^{28–30}. An accelerated pace might also result in earlier declines in brain plasticity, curtailing the development of cortical circuitry optimally suited to the environment^{31,32}. We have specifically posited that associations between disadvantage and the pace of structural brain development might be reflected in the trajectory of functional brain development: more protracted structural brain development observed in children with less exposure to disadvantage may give rise to a longer, slower trajectory of intrinsic cortical network segregation²². If so, children with less exposure to disadvantage should show more widespread connectivity and lower cortical network segregation early in development before the rapid development of a more segregated network architecture in later childhood and adolescence, leading to more effective cortical networks in adulthood due to protracted experience-dependent influences on network segregation²². Models drawn from evolutionary developmental frameworks also suggest that the early environment might be related to the pace of maturation. These models posit that early experiences tailor organisms to anticipated conditions in the future and suggest that harsh and unpredictable environments may be associated with life-history strategies resulting in accelerated development and early maturity, while safe and nurturing environments may result in prolonged developmental strategies and extended experience-dependent learning^{33–35}. Relatedly, the recent “change of tempo” model contends that different forms of adversity have different relations to pace: in situations of deprivation, such as inadequate nutrition or parental care, delaying maturation lowers children’s physiological requirements, while in the context of threat or abuse accelerated development may boost children’s ability to provide for immediate unmet safety needs³⁶. We recently proposed that experiences that are both negative and chronic are likely to accelerate brain development and reduce plasticity, while exposure to positive and rare or variable experiences are most likely to decelerate brain development and enhance plasticity²². At the same time, a recent review concluded that SES may simply be associated with alterations in brain development trajectories, not specific to pace, though the authors noted the dearth of studies on intrinsic brain network development³⁷. Limited empirical work has employed the longitudinal data necessary to model associations between disadvantage and trajectories of cortical network segregation, particularly in the earliest stages of life.

In this work, we explicitly test whether early disadvantage is associated with differences in the pace of intrinsic cortical network segregation during the first three years of life. We capitalize on a cohort of neonates and toddlers with longitudinal neuroimaging data and extensively characterized early environments¹⁹. Prenatal disadvantage was assessed using a latent factor of socioeconomic disadvantage that included measures of mother’s income-to-needs ratio, educational attainment, area deprivation index, insurance status, and nutrition. In this cohort, prenatal disadvantage is associated with brain structure and region-specific connectivity at birth^{38–40}, however, associations between prenatal disadvantage and whole-brain function or longitudinal brain development have not yet been examined. Here, we test the theory that prenatal disadvantage is associated with differences in the pace of functional brain network development, and that neonates and toddlers from more advantaged backgrounds might show a more protracted trajectory of cortical network segregation. In a set of pre-registered analyses, we examine the development of cortical network segregation during the first three years of life, and the moderating effects of prenatal disadvantage on trajectories of cortical network segregation. We find that developmental increases in cortical functional network segregation are accelerated in neonates and toddlers with greater exposure to prenatal disadvantage. We take a hierarchical approach, first examining measures of cortical network segregation at the whole brain resolution, then analyzing at the level of functional brain systems, and finally at the level of individual brain regions. Based on the hypothesis that age-dependent changes in cortical plasticity might result in regional variability in associations between prenatal disadvantage and cortical network segregation, we find that environmental effects are constrained by a sensorimotor-association cortical hierarchy, with the strongest associations present in early-developing sensory systems. Finally, we show that differences in measures of cortical network segregation at 2 years of age are associated with language and cognitive abilities at the same age.

Results

Cortical network segregation increases from birth to 3 years

We first investigated the maturation of cortical functional network architecture between birth and 3 years of age by examining measures of cortical network segregation. Cortical network segregation can be measured at different scales, ranging from the local, or regional, scale to the global, or whole-brain, scale (Fig. 1a–c). Global segregation captures the extent to which sets of systems in a cortical network are distinctly partitioned, while meso-scale segregation captures the extent to which a network can be divided into distinct subnetworks, and local segregation quantifies clustered connectivity at the regional or parcel level. We fit generalized additive mixed models (GAMMs) to measures of network segregation at each of these three levels, controlling for sex, amount of fMRI data included, in-scanner motion, and average network connectivity, and including a smooth term for age, where the smooth function (model fit for age) describes the relationship between cortical network segregation and age. Across scales, cortical network segregation increases with age. Global segregation, calculated from system segregation, increased with age (Fig. 1, $F_{s(\text{age})} = 6.26$, $\text{EDF} = 2.26$, $p = 0.001$, $p_{\text{FDR}} = 0.001$), as did meso-scale segregation ($F_{s(\text{age})} = 3.93$, $\text{EDF} = 1.90$, $p = 0.014$, $p_{\text{FDR}} = 0.014$), and local segregation ($F_{s(\text{age})} = 43.23$, $\text{EDF} = 2.33$, $p < 0.001$, $p_{\text{FDR}} < 0.001$), indicating increasing refinement of network architecture during early development.

Next, we probed the variation in the rate of change of cortical network segregation during the first three years of development. Here, the first derivative of the smooth function of age represents the rate of change in network segregation at a given developmental time point. Analysis of the derivatives of the age trajectories showed that measures of network segregation are increasing most strongly during the first two years of life. Global segregation increased between 0–1.93

years, meso-scale segregation increased between 0–1.70 years, and local segregation increased between 0–2.13 years, consistent with the most rapid change in cortical network segregation occurring early in development.

Prenatal disadvantage moderates trajectories of cortical network segregation

As described above, theoretical models posit that environmental influences on brain development might arise by way of effects on the pace of brain development, such that brain development proceeds faster in neonates and toddlers with greater exposure to disadvantage. To test this hypothesis, we examined associations between the early environment and developmental increases in cortical network segregation. We used GAMMs to formally model age-by-disadvantage interactions, which estimate how relationships between prenatal disadvantage, our measure of early environment, and network segregation vary continuously with age. We observed significant and similar patterns of interactions between prenatal disadvantage and age across multiple scales, such that infants and toddlers with greater exposure to prenatal disadvantage show a faster increase in cortical network segregation than infants and toddlers with less disadvantage, ending up at a higher level of network segregation. This pattern held true for global segregation (Fig. 2a, $F_{s(\text{age} \times \text{SES})} = 6.38$, $p = 0.002$, $p_{\text{FDR}} = 0.002$),

meso-scale segregation (Fig. 2b, $F_{s(\text{age} \times \text{SES})} = 9.86$, $p < 0.001$, $p_{\text{FDR}} = 0.001$), and local segregation (Fig. 2c, $F_{s(\text{age} \times \text{SES})} = 13.40$, $p < 0.001$, $p_{\text{FDR}} < 0.001$).

Intuitively, measures of network segregation at different scales will be related: segregation at the global scale will encompass segregation at both the meso (intermediate) scale and the local scale. Correspondingly, we observe that measures of segregation are correlated with each other (global segregation – meso-scale segregation: $t(417) = -6.51$, $p < 0.001$, $r = -0.30$, 95% CI = $[-0.39, -0.21]$; meso-scale segregation – local segregation: $t(417) = 19.11$, $p < 0.001$, $r = 0.68$, 95% CI = $[0.63, 0.73]$; local segregation – global segregation: $t(417) = 18.51$, $p < 0.001$, $r = -0.67$, 95% CI = $[-0.72, -0.62]$). To determine which effect drives the observed age-by-disadvantage associations with cortical network segregation, we conducted a series of analyses examining age-by-disadvantage associations with network segregation at each scale, controlling for network segregation at other scales. When we included average local segregation in the model for global segregation, age \times disadvantage no longer significantly predicts global segregation ($F_{s(\text{age} \times \text{SES})} = 2.62$, $p = 0.074$). The same is true when we included average local segregation in our model for meso-scale segregation: the age-by-disadvantage effect is no longer significant ($F_{s(\text{age} \times \text{SES})} = 0.76$, $p = 0.471$). The inverse is not the case – including meso-scale or global segregation in our model of local segregation does not affect the

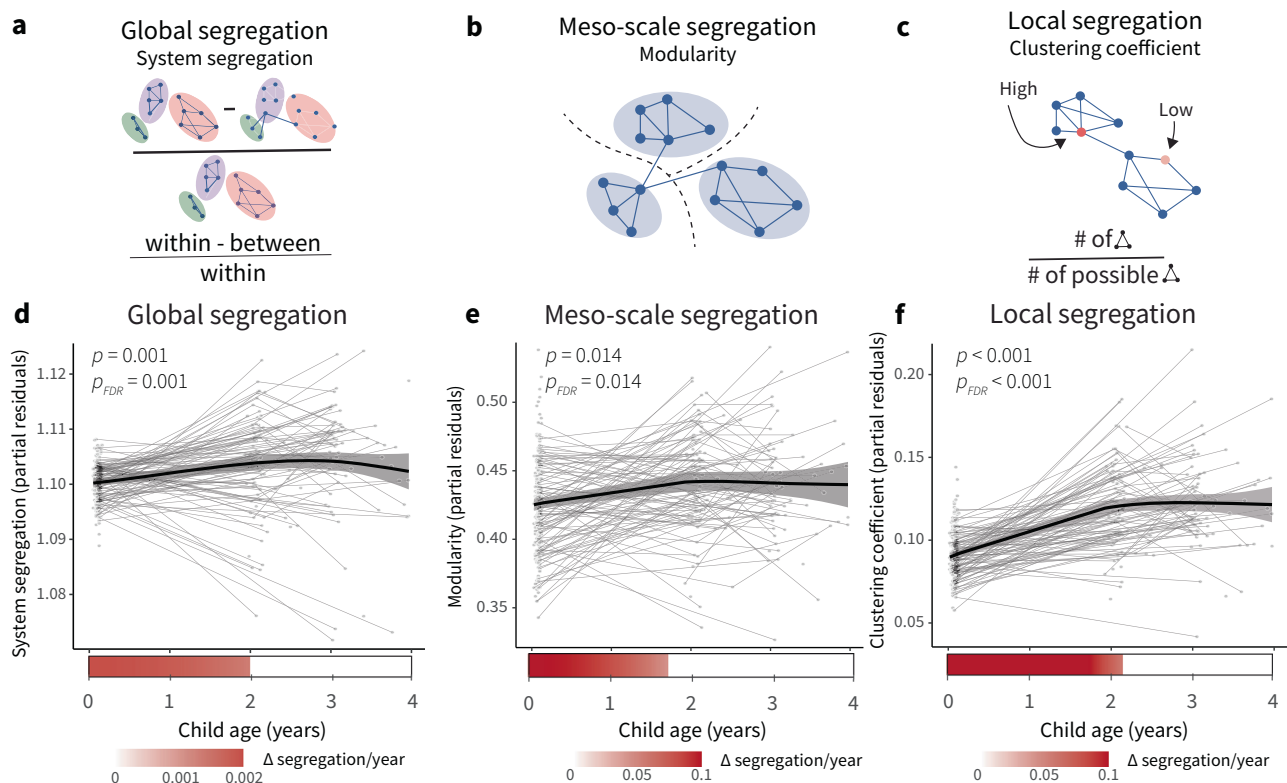


Fig. 1 | Cortical network segregation increases with age during the first three years of life. **a** System segregation is a whole-brain measure of functional network segregation that quantifies the difference between mean within-system connectivity and mean between-system connectivity as a proportion of mean within-system connectivity. **b** Modularity is a measure of network segregation that estimates the extent to which the nodes of a network, or in this case brain regions, can be subdivided into modules characterized by strong, dense intramodular connectivity and weak, sparse intermodular connectivity. Note that the modules are data driven, not a priori defined as functional systems. **c** The clustering coefficient is a measure of local segregation that quantifies the amount of connectivity between a node and its neighbors. A node has a high clustering coefficient when a high proportion of its neighbors are also strongly connected to one another. In a weighted network, the clustering coefficient measures the strength of triangles

around a node. **d** Global segregation increases significantly with age. **e** Meso-scale segregation increases significantly with age. **f** Local segregation increases significantly with age. Individual points represent individual scans, with lines indicating scans from the same participant. Analyses in (d–f) conducted using generalized additive mixed models (GAMMs), P values are FDR-corrected across models for changes in measures of cortical network architecture with age (Figs. 1d–f and 6b). Trajectories represent the GAMM-predicted segregation values with a 95% credible interval band. Bars below the x-axis depict the derivative of the fitted smooth function of age. The filled portion of the bar indicates periods where the magnitude of the derivative of the fitted curve is significant, with the saturation of the fill representing the value of the derivative. Panels a–c reprinted with permission from ref. 7.

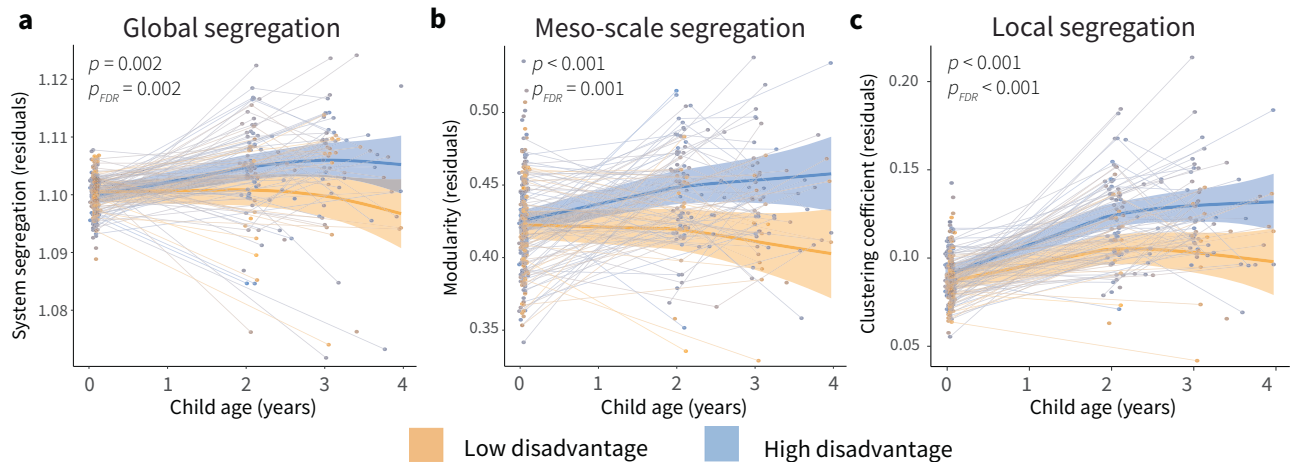


Fig. 2 | Associations between the early environment and developmental increases in cortical network segregation. **a** Prenatal disadvantage moderates trajectories of global cortical network segregation. **b** Prenatal disadvantage moderates trajectories of meso-scale cortical network segregation. **c** Prenatal disadvantage moderates trajectories of local cortical network segregation. Analyses in (a–c) conducted using generalized additive mixed models (GAMMs). *P* values are FDR-corrected across models for associations between prenatal disadvantage and developmental changes in cortical network architecture (Figs. 2a–c and 6c). Plots

display fitted network segregation trajectories from GAMM models plotted by age for participants from low prenatal disadvantage backgrounds (orange) and high prenatal disadvantage backgrounds (blue) with a 95% credible interval band. Disadvantage was modeled continuously; for visualization purposes here we show model trajectories from lowest and highest deciles of prenatal disadvantage. Individual points represent individual scans, with lines indicating scans from the same participant.

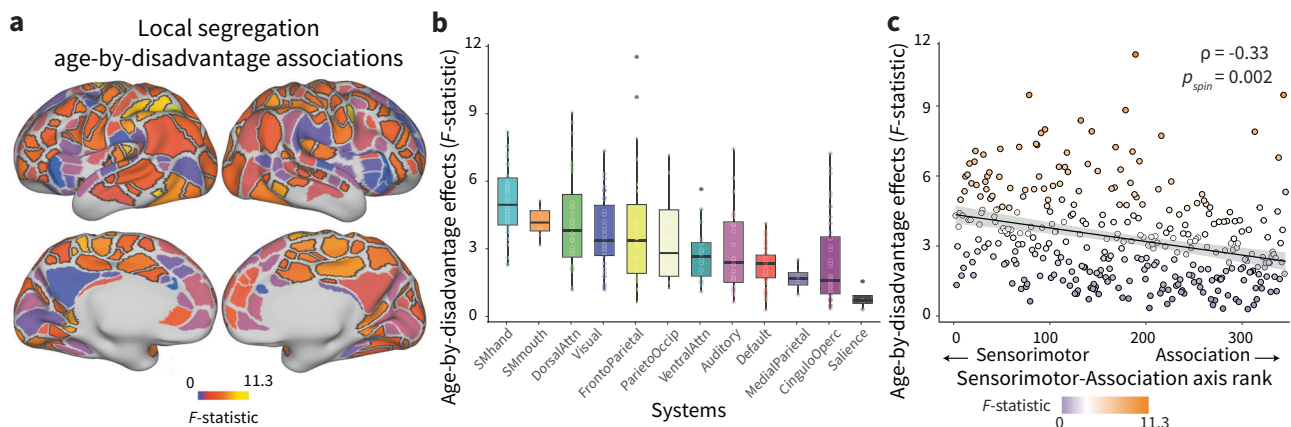


Fig. 3 | Associations between environment and developmental increases in local segregation are enriched in somatomotor systems. **a** The heterogeneous patterning of the magnitude of age-by-disadvantage associations (*F*-statistic) with local segregation is shown on the cortical surface. Regions that show significant age-by-disadvantage associations passing FDR correction at $p_{FDR} < 0.05$ are outlined in black. **b** Prenatal disadvantage associations with developmental increases in local segregation are enriched in somatomotor systems. Boxplots show the magnitude of age-by-disadvantage associations; each point is an individual parcel ($n = 286$ parcels, excluding parcels with system assignment None). Boxplots show median and 25–75% interquartile range; whiskers extend to $1.5 \times$ interquartile range,

points outside are shown as outliers. **c** The magnitude of age-by-disadvantage associations is related to a canonical sensorimotor-to-association axis of cortical organization. Each point is an individual parcel, the color of the points represents the magnitude of age-by-disadvantage association. A Spearman's correlation between these two measures assessed by a conservative two-sided spin-based rotation test was significant ($\rho(331) = -0.33$, $p_{spin} = 0.002$, 95% CI = $[-0.43, -0.24]$). The predicted negative linear relationship between these two measures is plotted with a 95% confidence interval, colors of the points correspond to the magnitude of age-by-disadvantage associations with regional local segregation.

significance of the age-by-disadvantage interaction (global segregation: $F_{s(\text{age} \times \text{SES})} = 9.46$, $p < 0.001$; meso-scale segregation; $F_{s(\text{age} \times \text{SES})} = 4.60$, $p = 0.011$). Therefore, we concluded that the fundamental driver of the age-by-disadvantage associations is variation in local network topology, as indexed by our measure of local segregation. Thus, in the analyses that follow we focus specifically on local segregation and associated variation in local network architecture.

Prenatal disadvantage associations are strongest in somatomotor and dorsal attention systems

To characterize associations between the environment and cortical network development in individual cortical regions, we conducted a

series of exploratory (not pre-registered) analyses. We fit region-specific GAMM models to regional measures of local segregation, including a smooth term for age, and allowing age to interact with prenatal disadvantage. A total of 56% of regions showed significant age-by-disadvantage associations with local segregation, indicating that moderating associations between the environment and cortical network development are widespread across the cortex ($p_{FDR} < 0.05$, Fig. 3a). To provide insight into the magnitude of moderating associations with prenatal disadvantage across cortical regions, we calculated the magnitude of variance explained by the addition of the age-by-disadvantage interaction (*F*-statistic). The magnitude of associations between prenatal disadvantage and

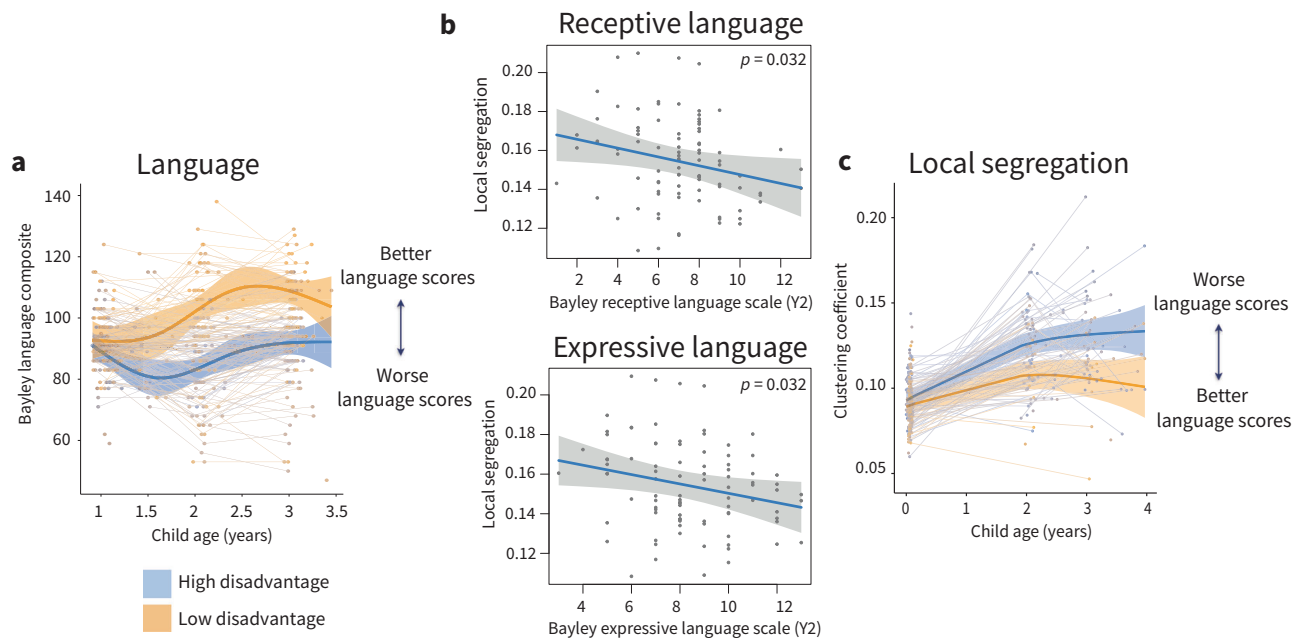


Fig. 4 | Associations between local cortical network segregation and language abilities at age 2 years. **a** Associations between prenatal disadvantage and trajectories of age-standardized Bayley language composite scores. Disadvantage was modeled continuously, for visualization purposes here we show model trajectories from lowest and highest deciles of prenatal disadvantage with a 95% credible interval band. Individual points represent scores from individual participants, with lines indicating data collected from the same participant. **b** Local segregation at 2 years of age was negatively associated with scores on both expressive and receptive

language subscales. Analyses conducted using linear multiple regression models. Scores on the receptive and expressive language subscales had different ranges, with children scoring slightly higher on the expressive language scale (x-axis). **c** The directionality of this association is such that higher levels of local segregation, which are found in toddlers with greater exposure to prenatal disadvantage, are associated with worse performance on measures of language ability. Trajectories represent the GAMM-predicted segregation values with a 95% credible interval band.

developmental increases in local segregation differed across the cortex, signifying that there is variability in the association between the early environment and cortical network maturation across the developing cortex.

To better understand the pattern of variability in associations with the environment across the cortex, we asked whether moderating associations between prenatal disadvantage and age-related increases in local segregation might be more pronounced in specific functional systems. The magnitude of associations between prenatal disadvantage and developmental increases in local segregation differed across functional systems ($H(12) = 90.413$, $\eta^2_H = 0.25$, $p < 0.001$, 95% CI = [0.19, 0.36]), with the strongest associations found in somatomotor-hand, somatomotor-mouth, dorsal attention, visual, and frontoparietal systems (Fig. 3b), consistent with environmental associations with cortical network development being most pronounced in early-developing sensorimotor regions during the first years of life. We wondered whether this was an overall principle of associations between the early environment and cortical network development, so we examined the correspondence between associations between prenatal disadvantage and developmental increases in local segregation and a canonical axis of sensorimotor-association cortical organization⁸. Age-by-disadvantage associations with local segregation were negatively correlated with sensorimotor-association axis ranks across regions (Fig. 3c, $\rho(331) = -0.33$, $p_{\text{spin}} = 0.002$, 95% CI = [-0.43, -0.24]), with larger environmental associations with developmental increases in local segregation characterizing the S-A axis's sensorimotor pole, and smaller, near zero associations at the association pole.

Associations between cognition and disadvantage-associated differences in local segregation

Finally, we sought to understand whether associations between the environment and the development of cortical network segregation

relate to differences in language and cognition that we observe later in development. Disadvantage-associated differences in language (Fig. 4a, $F_{s(\text{age} \times \text{SES})} = 7.54$, $p < 0.001$, $p_{\text{FDR}} < 0.001$) and cognitive ($F_{s(\text{age} \times \text{SES})} = 12.65$, $p < 0.001$, $p_{\text{FDR}} < 0.001$) composite scores are evident from 2 years of age. Thus, we examined whether differences in local segregation at 2 years, when we first observe diverging trajectories of cortical network segregation associated with prenatal disadvantage, were associated with language or cognition composite scores at the same time point. There was no statistically significant association between average whole-cortex local segregation and cognition scores ($t(83) = -0.30$, $p = 0.766$, $p_{\text{FDR}} = 0.766$, $\beta = -0.03$, 95% CI = $[-5.66 \times 10^{-4}$, $-4.18 \times 10^{-4}]$). Average whole-cortex local segregation was negatively associated with language scores (Fig. 4b, $t(83) = -2.45$, $p = 0.017$, $p_{\text{FDR}} = 0.033$, $\beta = -0.23$, 95% CI = $[-8.84 \times 10^{-4}$, $-9.12 \times 10^{-5}]$), indicating that lower levels of cortical network segregation seen in less disadvantaged toddlers are associated with better language abilities at 2 years of age. Importantly, when examining year two language ability and additionally controlling for prenatal disadvantage, we find that both prenatal disadvantage ($t(83) = -2.26$, $p = 0.027$, $\beta = -0.23$, 95% CI = $[-6.72$, $-0.42]$) and average local segregation ($t(83) = -2.43$, $\beta = -0.25$, $p = 0.017$, 95% CI = $[-217.38$, $-21.59]$) are significantly associated with language scores, indicating that cortical network segregation is independently associated with language ability at 2 years, above and beyond the association between early disadvantage and later language abilities.

We examined whether associations between local segregation and language abilities were driven by the receptive or expressive language subscales of the language composite and found that local segregation was negatively associated with both expressive (Fig. 4c, $t(83) = -2.19$, $\beta = -0.21$, $p = 0.032$, 95% CI = $[-4.52 \times 10^{-3}$, $-2.13 \times 10^{-4}]$) and receptive language abilities ($t(83) = -2.18$, $\beta = -0.21$, $p = 0.032$, 95% CI = $[-4.34 \times 10^{-3}$, $-1.97 \times 10^{-4}]$). When controlling for prenatal disadvantage, local segregation was associated with receptive language

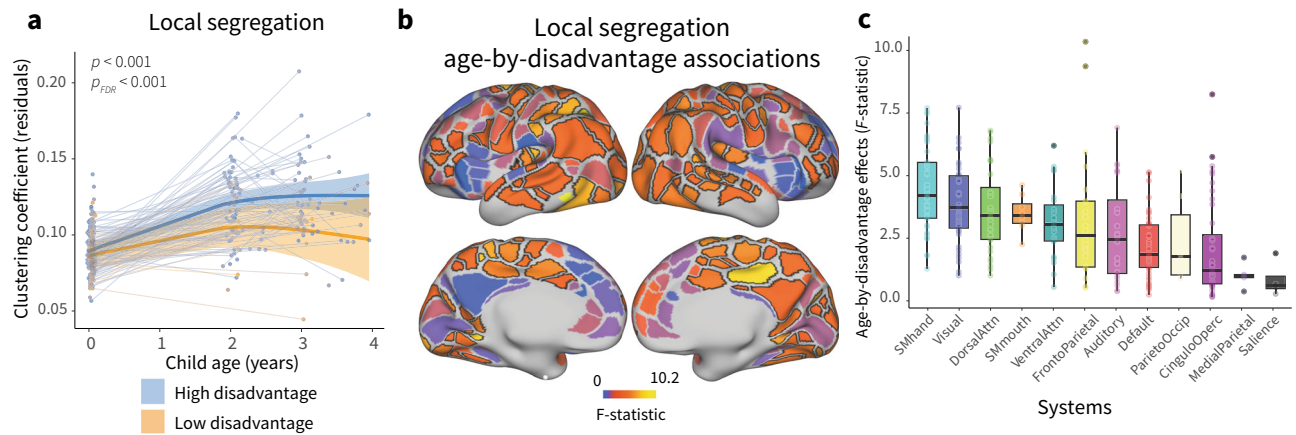


Fig. 5 | Associations between a composite measure of SES (maternal education and income-to-needs ratio) and developmental increases in cortical network segregation. **a** Prenatal disadvantage moderates trajectories of local cortical network segregation. Analyses conducted using generalized additive mixed models (GAMMs). *P* values are FDR-corrected across models for associations between prenatal SES and developmental changes in cortical network architecture. Trajectories represent the GAMM-predicted segregation values with a 95% credible interval band. **b** The heterogeneous patterning of the magnitude of age-by-

disadvantage associations (*F*-statistic) with local segregation is shown on the cortical surface. Regions that show significant age-by-disadvantage associations passing FDR correction at $p_{\text{FDR}} < 0.05$ are outlined in black. **c** SES associations with developmental increases in local segregation are enriched in sensorimotor systems. Boxplots show the magnitude of age-by-disadvantage effects; each point is an individual parcel ($n = 286$ parcels, excluding parcels with system assignment None). Boxplots show median and 25–75% interquartile range; whiskers extend to 1.5 * interquartile range, points outside are shown as outliers.

($t(83) = -2.33$, $\beta = -0.25$, $p = 0.022$, 95% CI = $[-41.75, -3.26]$), but there was no statistically significant association with expressive language ($t(83) = -1.96$, $\beta = -0.21$, $p = 0.053$, 95% CI = $[-36.16, 0.24]$).

While our sample size was reduced at the 3-year timepoint due to COVID-related limitations in data collection ($n = 90$ at year two, $n = 66$ at year three), we additionally examined whether differences in local segregation at age 3 years were associated with language or cognition composite scores. We found a similar pattern of effect sizes at the 3-year timepoint, with average local segregation negatively associated with language scores ($t(83) = -2.84$, $\beta = -0.33$, $p = 0.006$, $p_{\text{FDR}} = 0.012$, 95% CI = $[-0.001, -1.84 \times 10^{-4}]$), but not cognitive scores ($t(83) = -1.67$, $\beta = -0.20$, $p = 0.100$, $p_{\text{FDR}} = 0.100$, 95% CI = $[-0.001, 0.0001]$). Local segregation was negatively associated with both receptive ($t(83) = -2.45$, $\beta = -0.29$, $p = 0.015$, 95% CI = $[-5.34 \times 10^{-3}, -5.90 \times 10^{-4}]$) and expressive language abilities ($t(83) = -2.94$, $\beta = -0.35$, $p = 0.005$, 95% CI = $[-6.32 \times 10^{-3}, -1.20 \times 10^{-3}]$). When controlling for prenatal disadvantage at the 3-year timepoint, we find similar effect sizes for associations between local segregation and language scores as at age 2 years, but neither associations with the language composite ($t(83) = -1.50$, $\beta = -0.19$, $p = 0.138$, 95% CI = $[-235.92, 33.31]$), or the expressive ($t(83) = -1.38$, $\beta = -0.17$, $p = 0.173$, 95% CI = $[-39.37, 7.21]$) or receptive ($t(83) = -1.46$, $\beta = -0.19$, $p = 0.148$, 95% CI = $[-44.15, 6.83]$) language scales are significant (Fig. 4c).

Disadvantage associations with developmental increases in cortical network segregation are robust to methodological variation

To ensure that the environmental associations with changes in cortical network segregation observed were robust to methodological variation and potential confounds, we performed five sensitivity analyses. We first conducted one of our pre-registered follow-up analyses, and evaluated whether associations between prenatal disadvantage and developmental increases in cortical network segregation were accounted for by an alternate measure of the early environment. In this analysis, GAMMs were rerun with a composite SES measure of income-to-needs ratio (INR) and maternal education at birth rather than the prenatal disadvantage factor score (i.e., excluding neighborhood disadvantage, diet, and insurance status). When using this composite measure of SES, global segregation ($F_{s(\text{age} \times \text{SES})} = 3.74$, $p = 0.024$, $p_{\text{FDR}} = 0.033$), meso-scale segregation ($F_{s(\text{age} \times \text{SES})} = 7.78$, $p < 0.001$,

$p_{\text{FDR}} < 0.001$), and local segregation (Fig. 5a, $F_{s(\text{age} \times \text{SES})} = 11.61$, $p < 0.001$, $p_{\text{FDR}} < 0.001$) all show significant and similar patterns of interactions, such that infants and toddlers with greater exposure to prenatal disadvantage show a faster increase in cortical network segregation than infants and toddlers with less disadvantage. The magnitude of SES associations with developmental increases in local segregation continued to vary across the cortex (Fig. 5b), with the strongest associations found in somatomotor-hand, visual, dorsal attention, and somatomotor-mouth systems (Fig. 5c).

We also evaluated whether associations between prenatal disadvantage and developmental increases in cortical network segregation were accounted for by differences in sample composition over the study period, alterations in functional network architecture associated with head motion, changes in disadvantage over the study period, longitudinal modeling choices, or outliers. In each sensitivity analysis, associations between the environment and developmental increases in cortical network segregation closely mirrored those observed in the main analysis, with neonates and toddlers with greater exposure to prenatal disadvantage showing a steeper increase in cortical functional network segregation than those with less exposure to disadvantage, and environmental associations with developmental increases in cortical network segregation enriched in sensorimotor systems (see Supplementary Note 1 and Figs. 1–5). We additionally examined whether there were associations between prenatal psychosocial stress independent of prenatal disadvantage and developmental changes in cortical network segregation, however, no significant associations were found (see Supplementary Note 1 and Fig. 6). These analyses verify that findings concerning the nature and patterning of environmental associations with developmental changes in cortical functional network segregation are robust to methodological variation.

No statistically significant environmental associations with age-associated changes in network integration

The previous analyses focused on developmental trajectories of network segregation, but another property of cortical network architecture that changes markedly as children develop is cortical network integration. Cortical network integration refers to the extent to which information can be integrated across multiple brain systems, and high levels of both network integration and network segregation together constitute the unique property of small-worldness found in adult brain

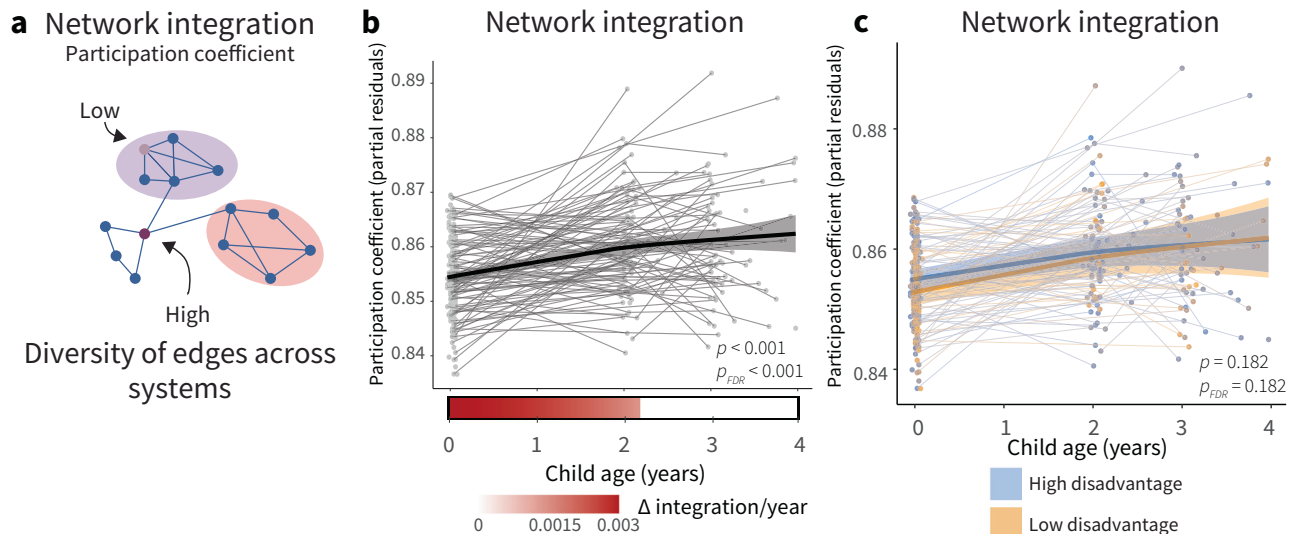


Fig. 6 | Null evidence for environmental associations with age-associated changes in network integration. **a** The participation coefficient is a measure of network integration that quantifies the diversity of the connections of a node. A node has a high participation coefficient when it is evenly connected to many different systems. Reprinted with permission from ref. 7. **b** Network integration increases significantly with age. Analyses conducted using generalized additive mixed models (GAMMs), P values are FDR-corrected across models for changes in measures of cortical network architecture with age (Figs. 1d–f and 6b). Individual points represent individual scans, with lines indicating scans from the same

participant. Bars below the x-axis depict the derivative of the fitted smooth function of age. The filled portion of the bar indicates periods where the magnitude of the derivative is significant, with the saturation of the fill representing the value of the derivative. **c** Prenatal disadvantage does not significantly moderate age-related increases in network integration. P values are FDR-corrected across models for associations between prenatal disadvantage and developmental changes in cortical network architecture (Figs. 2a–c and 6c). Trajectories represent the GAMM-predicted segregation values with a 95% credible interval band.

networks⁴¹. Thus, we also pre-registered examining developmental changes in and age-by-disadvantage associations with cortical network integration, as assessed by the average whole-brain participation coefficient. The participation coefficient is a measure of network integration that quantifies the diversity of the connections of a node across systems⁴², and has been linked in older children and adolescents to developmental changes in network segregation^{7,43,44} (Fig. 6a).

As previously, we fit a GAMM to average whole-cortex network integration with a smooth term for age, where the smooth function (model fit for age) describes the relationship between network integration and age. Average network integration increased with age (Fig. 6b, $F_{s(\text{age})} = 14.11$, $\text{EDF} = 1.68$, $p < 0.001$, $p_{\text{FDR}} < 0.001$), with the period of significant change occurring from birth to 2.27 years, consistent with the most rapid change occurring early in development. We found no statistically significant association between prenatal disadvantage and developmental changes in network integration (Fig. 6c, $F_{s(\text{age} \times \text{SES})} = 1.71$, $p = 0.182$, $p_{\text{FDR}} = 0.182$) in these primary analyses nor in supplemental analyses examining the alternative composite measure of disadvantage described above ($F_{s(\text{age} \times \text{SES})} = 1.53$, $p = 0.118$, $p_{\text{FDR}} = 0.118$).

Discussion

The first years of life are a critical window during which the development of the cortex proceeds in a heterochronous manner: sensory and motor cortices mature earlier than association cortices, and hierarchical refinement of plasticity-regulating features produces declines in the malleability of the cortex to environmental input, suggesting that the early environment may have a disproportionate effect on the pace of cortical development. In the current work, we show that the development of cortical brain networks during the first three years of life is strongly associated with features of the early environment, suggesting these influences may play a key role in shaping this trajectory. Specifically, we observe that developmental increases in cortical functional network segregation are accelerated in neonates and toddlers with greater exposure to prenatal disadvantage.

Environmental associations with the development of cortical network segregation conform to a sensorimotor-association hierarchy of cortical organization, with the strongest associations visible in early-developing somatosensory systems that have high plasticity during this period. Differences in cortical functional network segregation associated with the early environment are also associated with language abilities at age 2 years when controlling for prenatal disadvantage.

We find that being born into a more advantaged environment is associated with a more protracted trajectory of cortical functional network development in toddlerhood and early childhood, and our robustness analyses suggest that these effects are primarily driven by variation in socioeconomic factors. Prior work has found that differences in intrinsic functional connectivity associated with SES are evident at 6 months of age²⁴. Lower levels of cortical network segregation in children from more advantaged backgrounds at 3 years of age are also consistent with our earlier work in adolescents, where children from higher-SES backgrounds had lower levels of cortical network segregation at age 8 years²⁰. This underscores the possibility that being born into a more advantaged household may be associated with more protracted cortical functional network development throughout childhood, with children from more advantaged backgrounds showing more widespread connectivity and thus lower segregation early in development before the rapid development of a more segregated network architecture occurring during adolescence and into adulthood²². Experiences associated with disadvantage may result in earlier declines in plasticity in a heterogeneous and spatially patterned manner across the cortex. For example, one study using a putative measure of plasticity to probe how developmental variation in intrinsic cortical activity is associated with the environment finds that lower neighborhood SES is associated with reduced intrinsic activity, suggestive of decreased plasticity, in association cortex during adolescence⁴⁵. Earlier reductions in plasticity associated with disadvantage might thereby result in decreased synaptic proliferation^{46,47} or alterations in the development of inhibitory interneurons^{48,49}, as has

been found in animal models of early environmental stress, resulting in decreased range for optimal synaptic pruning and wiring of segregated cortical networks. In our cohort, neonates from more advantaged backgrounds show increased mean diffusivity, a measure of white matter microstructure, at birth compared to neonates from less advantaged backgrounds⁵⁰. As this measure of white matter microstructure typically decreases with age⁵¹, we speculate that this pattern could be indicative of more protracted white matter development in neonates from more advantaged backgrounds; accelerated development associated with higher advantage might be observable in both intrinsic cortical network segregation and also the white matter connectivity that supports intrinsic brain activity, questions that can be explored in future work.

We find that alterations in cortical network segregation associated with prenatal disadvantage are driven fundamentally by effects at the local scale. Associations between cortical network segregation and SES in older children and adolescents are also driven by alterations in local network architecture²⁰. In youth and adolescents, associations between household SES and local segregation are evident in the prefrontal cortex specifically among youth living in low-SES neighborhoods, more evidence for environmental influences at the local scale during development²¹. However, adulthood SES is associated with aging-associated declines in global segregation^{52,53}, thus one possibility is that associations between disadvantage and cortical network segregation follow a progression from local to global across the lifespan. However, the authors did not examine local or meso-scale measures of segregation, so this possibility has not yet been directly addressed; more work is needed to clarify the scale of environmental effects on measures of cortical network segregation.

We find that environmental associations with the development of cortical functional network segregation conform to a sensorimotor-association hierarchy of cortical organization, with the strongest associations with early environment visible in early-developing somatosensory systems, specifically, somatomotor, dorsal attention, and visual systems, with the frontoparietal system also showing strong environmental associations. While the dorsal attention system may not canonically be considered an early-developing system, dorsal attention regions mature dramatically between birth and 2 years of age⁵, are structurally and functionally connected to visual cortex^{34,55}, and fall at the unimodal end of the primary gradient of macroscale cortical organization⁵⁶. Environmental associations with cortical network segregation aligning with the sensorimotor-association hierarchy is consistent with a model where age-dependent changes in cortical plasticity allow environment effects to exert differential inputs on the human brain, depending on developmental timing, such that early plasticity in primary sensory regions allows for the largest environmental associations with intrinsic cortical activity in these regions during the first years of life.

Accumulating evidence from large-scale studies of older children and adolescents also suggests another possibility: environmental effects may be transduced through lower-level sensory systems, such that regardless of developmental stage, the strongest associations between the environment and intrinsic cortical activity are visible in somatosensory systems⁵⁷. Across multiple indicators of household and neighborhood disadvantage, strong associations between disadvantage and measures of functional connectivity are consistently found in somatomotor systems in children ages 9–11 years of age^{58–61}. In youth and adolescents ages 8–21 years, associations between SES and age-associated increases in cortical network segregation are also evident in somatomotor cortex²⁰. It is also possible that due to the low level of social mobility in the United States population from which these studies were drawn^{62,63}, socioeconomic position later in development measured in these studies is nearly identical to a participant's socioeconomic position at birth, and thus the disadvantage associations measured are simply long-lasting instantiations of the effects of

the birth environment on early-developing functional brain systems. Alternatively, brain areas at the sensorimotor pole of the S-A axis show the lowest variability between individuals^{64,65}, and thus may enable the detection of effects above and beyond interindividual variability. While environmental associations were most prominent in the somatomotor system, we also observe associations between the early environment and cortical network development in the frontoparietal system. Interestingly, the environmental associations observed in the frontoparietal system are driven by strong age-by-disadvantage interaction effects in regions in the intraparietal sulcus and middle temporal gyrus, rather than in lateral prefrontal regions, suggestive of alignment with an anterior-to-posterior developmental axis.

We find that disadvantage-associated differences in cortical functional network segregation are also associated with language abilities at age 2 years, suggesting that environmental associations with the development of cortical network segregation might underlie disadvantage-associated differences in language abilities observed later in development. The association between cortical network segregation and language abilities holds even when controlling for prenatal disadvantage, suggesting that cortical network segregation is associated with language ability independent of the well-documented association between early disadvantage and later language ability. While to our knowledge no other studies have specifically examined associations between cortical network segregation and language during early development, one study of toddlers and children ages 0–6 years found that increased between-system connectivity was associated with better language performance⁶⁶, and infants with more language interactions had lower within-system connectivity in the language system⁶⁷. Both findings potentially indicate that better language performance and more language exposure may be associated with lower levels of network segregation. The directionality of associations between cortical network segregation and language ability we find in toddlers is broadly reversed compared with associations found in adolescents and adults, where higher levels of cortical network segregation have been found to be advantageous for language and cognition^{9,11,12}. During late childhood, children from higher SES backgrounds show lower levels of cortical network segregation, but by early adulthood, higher SES is associated with higher cortical network segregation²⁰, suggesting that initially low cortical network segregation might be beneficial for the development of cognitive and language abilities associated with higher SES (lower disadvantage)¹⁵. However, the directionality of associations between cortical network segregation and behavior in adults also varies based on life stage and behavioral domain examined^{6,10,68}, underscoring the importance of understanding developmental trajectories and domain specificity when interpreting the directionality of associations.

There are several possible mechanisms by which variation in the early environment could signal to alter the tempo of brain development. One commonly proposed mechanism is deprivation, where lack of expected inputs at a developmental stage results in earlier pruning of synapses and reduced synaptic connectivity^{69,70}. Recently, we put forth a model in which the valence and variability of experiences interact to predict maturational pace, such that experiences that are chronic and negative encourage faster maturation and restrict plasticity, and experiences that are novel and positive delay maturational processes and enhance plasticity²². Growing up in a more advantaged environment is associated with more cognitively enriching, positively valenced experiences⁷¹. This environment—the opposite of deprivation⁶⁹—may delay maturational processes and prolong plasticity: animals exposed to enriched environments as juveniles display enhanced markers of synaptic and extracellular markers of plasticity^{72,73}, and the release of neurotransmitters associated with positive experiences increases cortical plasticity and facilitates remodeling^{74–76}. Conversely, negative experiences such as stress might accelerate brain development through several different

mechanisms^{77–79}; higher disadvantage is consistently associated with higher stress⁸⁰. Although in this work we find that prenatal socioeconomic disadvantage has stronger effects on brain development than does psychosocial stress, our measurement of stress was limited; stress may still be one of several mechanisms by which prenatal disadvantage results in changes in the tempo of brain development.

The variability of experiences might also interact with the valence of experiences to predict maturational pace. Repeated exposure to the same experience, signaling to the brain to optimize for the continued occurrence of this experience in the future, can accelerate maturation of specific circuitry^{81–83}. This aligns with theories of stress effects on maturational pace, where repeated stress-detection and stress-regulation leads to faster maturation of the amygdala and medial prefrontal cortex^{77,84}. In contrast, rare or highly variable experiences could signal that the environment is still changing, and that plasticity is beneficial⁸⁵. Computational evolutionary models suggest that individuals who have more variable experiences lose plasticity later in development than those with more consistent experiences^{86–88}, and some evidence from the study of critical periods suggests that periods of plasticity are prolonged when environmental statistics are variable or unreliable^{89,90}. Further work testing these models and delineating which dimensions are most important contributors to the observed effects of the early environment on the pace of brain development will be key to understanding the mechanisms by which environmental cues give rise to changes in maturational tempo.

Several limitations and possible direct extensions of this work should be highlighted. First, it is important to acknowledge that socioeconomic disadvantage is but one form of disadvantage, and other forms not examined here, such as discrimination and systemic racism, may also be associated with brain development^{91,92}. Different environmental exposures associated with disadvantage – such as stress, cognitive stimulation, and unpredictability—are associated with brain development differently^{70,77,93,94}, and differentiating the relative contributions of these associated exposures to the effects that we observe is a critical and urgent future direction. Second, due to the impact of the COVID-19 pandemic, sample sizes at the toddler timepoints were smaller than originally intended, and thus our analyses of behavior at the 2- and 3-year time points should be considered exploratory; we share them as grounds for future work on the topic. Third, we employed a common adult parcellation and set of systems to characterize cortical network development. It is possible that differences in the degree to which a neonate's fine-grained cortical topography resembles that of an adult might influence measures of cortical network segregation; the continued development of neonatal parcellations^{55,96} will enable future work to use infant-specific parcellations and systems to characterize brain development. Fourth, here we focus specifically on changes in intrinsic cortical networks during postnatal development, but environmental factors also impact prenatal brain development; future work should investigate mechanisms of associations between the prenatal environment and cortical networks. Finally, while we observed associations between cortical intrinsic network development and language during toddlerhood, accelerated cortical network development may also have implications for the development of cognition and psychopathology that only become evident later in childhood. Longitudinal data from birth to middle childhood on both brain and behavioral development will be necessary to answer this question, data which will fortunately soon be available in the HEALTHY Brain and Child Development (HBCD) study⁹⁷.

The present study demonstrates that the development of intrinsic cortical brain networks during the first three years of life is associated with features of the early environment. The observed effects are consistent with an interpretation of accelerated cortical functional network development during the first years of life in neonates and toddlers exposed to greater prenatal disadvantage. Insight into the timing and directionality of environmental associations with

trajectories of cortical brain development are crucial elements for understanding the optimal timing for interventions, to prevent cascading consequences of early maturation. Our results emphasize the importance of expanding and enhancing policies that provide financial support to parents of young children^{98–101}.

Methods

Participants

Neonates were recruited as a part of the Early Life Adversity, Biological Embedding, and Risk for Developmental Precursors of Mental Health Disorders (eLABE) cohort¹⁹, whose participants were recruited under the parent March of Dimes study¹⁰². Pregnant mothers were recruited and enrolled between the second and third trimesters. Recruitment oversampled mother-infant pairs facing adversity (e.g., poverty and stress). Inclusion criteria for the study included speaking English, mother age 18 years or older, and singleton birth (see Supplementary Table 1 for detailed participant information). Women with alcohol or other substance abuse were excluded. Anatomic MR images were reviewed by a neuroradiologist (J.S.S.) and pediatric neurologist (C.D.S.). Subjects were excluded from the current analyses if they had evidence of brain injury or were born preterm (<37 weeks gestational age, GA). Additional exclusion criteria included pregnancy complications (but not gestational diabetes or hypertension) and known fetal abnormalities including intrauterine growth restriction. This study was approved by the Human Studies Committees at Washington University in St. Louis and informed consent was obtained from a parent of all participants. Participants were compensated \$100–\$300 per study visit at each timepoint: participants were compensated \$100 for scans at the neonatal timepoint and \$125 for scans at 2-year and 3-year timepoints, \$100 for completion of assessments at each timepoint, and \$50–100 for completion of survey measures at each timepoint.

At each timepoint, all participants with usable functional magnetic resonance imaging (fMRI) and demographic data were included. No statistical method was used to predetermine sample size. At the neonatal timepoint, 385 neonates were scanned, and participants were excluded from all timepoints for the following reasons: <37 weeks GA at birth ($n = 54$), brain injury ($n = 17$), neonatal intensive care unit stay for >7 days, required intubation or chest tube, antibiotics for >3 days, cardiac disease or metabolic disorder ($n = 36$), birthweight <2000 g ($n = 1$), and IRB exclusion ($n = 1$). There were 306 participants who did not meet any of these exclusion criteria (note that some met multiple exclusion criteria).

Of these participants, 261 participants (age range = 38–45 post-menstrual weeks, $M = 41.3$ months, 54% male) were included in the current analyses at the neonatal timepoint. Neonates were excluded for no usable T2 for registration ($n = 27$), no functional magnetic resonance imaging (fMRI) data collected or <10 min of usable fMRI data after motion censoring ($n = 12$), or visible artifacts in FC data ($n = 7$).

At the 2-year timepoint, 202 participants were scanned, of which 162 were healthy full-term neonates not subject to the exclusions above. Participants were additionally excluded for no usable T1 for registration ($n = 68$) or no functional magnetic resonance imaging (fMRI) data collected ($n = 2$), resulting in 92 participants (range = 1.91–2.61 years, $M = 2.11$ years, 59% male) included at year two. At the 3-year timepoint, 132 participants were scanned, of which 98 were healthy full-term neonates. Participants were additionally excluded for no usable T1 for registration ($n = 31$) or <5 min of usable fMRI data after motion censoring ($n = 1$) resulting in 66 participants included from year 3 (range = 2.92–3.97 years, $M = 3.22$ years, 64% male).

Participants who returned for data collection at year two were not significantly different than participants from whom we were not able to collect year two data in gestational age, birthweight, prenatal disadvantage, psychosocial stress, sex, neighborhood deprivation, or income-to-needs ratio (two-sided t -test, all p 's > 0.05). Participants

who returned for data collection at year three were significantly more advantaged (lower prenatal disadvantage, $t(358) = -2.42$, $p = 0.016$) than participants from whom we were not able to collect year three data; there were no other significant differences between groups (p 's > 0.05).

MRI data acquisition

Imaging was performed without sedating medications at all three time points using a 3 T Prisma scanner (Siemens Corp.) and 64-channel head coil. During the scan session, structural images were collected: a T2-weighted image at the neonatal timepoint (sagittal, 208 slices, 0.8-mm isotropic resolution, echo time, TE = 563 ms, repetition time, TR = 3200 ms) and a T1-weighted image at the 2- and 3-year timepoints (sagittal, 208 slices, 0.8-mm isotropic resolution, repetition time = 2400 ms, echo time = 2.22 ms). Resting-state functional imaging data (fMRI) were collected using a blood oxygen level-dependent (BOLD) gradient-recalled echo-planar multiband sequence (72 slices, 2.0-mm isotropic resolution, echo time = 37 ms, repetition time = 800 ms, multiband factor = 8, 420 volumes). Spin-echo field maps were obtained (at least 1 anterior-posterior and 1 posterior-anterior) during each session with the same parameters. Between 2 and 9 5.6 min fMRI BOLD scans were acquired, depending on how the child tolerated the scan (range = 7.5–44.8 min). Framework Integrated Real-time MRI Monitoring (FIRMM^{103,104}) was used during scanning to monitor real time participant movement.

MRI data preprocessing

fMRI preprocessing included correction of intensity differences attributable to interleaved acquisition, bias field correction, intensity normalization of each run to a whole-brain mode value of 1,000, linear realignment within and across runs to compensate for rigid body motion, and linear registration of BOLD images to the adult Talairach isotropic atlas. Neonates were registered: BOLD to individual T2 to group-average T2 from this cohort to 711-2 N Talairach atlas. Toddlers were registered: BOLD to individual T1 to group-average T1 from this cohort to 711-2 N Talairach atlas. Field distortion correction was performed, using the FSL 6.0.4 TOPUP toolbox (<http://fsl.fmrib.ox.ac.uk/fsl/fslwiki/TOPUP>). Functions from the 4dfp analysis suite v0.1.0 were used for preprocessing (<https://4dfp.readthedocs.io/en/latest/>). Following initial processing, frames contaminated by motion were censored as described below. A surface-based neonatal parcellation approach, Melbourne Children's Regional Brain Atlases (MCRIB), was used to generate surfaces for each neonatal subject and the volumetric resting-state BOLD timeseries were mapped to subject-specific surfaces using established procedures adapted from the Human Connectome Project as implemented in Connectome Workbench 1.2.3. Freesurfer 7.2 was used to generate surfaces for each toddler subject, and the volumetric resting-state BOLD timeseries were mapped to subject-specific surfaces using identical procedures adapted from the Human Connectome Project as implemented in Connectome Workbench 1.2.3.

After mapping to the surface, each dataset underwent resting-state fMRI preprocessing. Data were processed with the following steps: (i) nuisance regression including white matter, ventricles, extra-axial cerebrospinal fluid, and whole brain, as well as 24-parameter Friston expansion regressors derived from head motion, and (ii) band-pass filtering (0.005 Hz $< f < 0.1$ Hz) with demean and detrend within-run, interpolating censored frames within run.

Neonatal fMRI data were censored at $FD > 0.25$ mm, with the additional restriction that only epochs of at least 3 consecutive frames $FD < 0.25$ mm were included. This FD threshold was selected after taking into account the smaller radius of infants' heads¹⁰⁵ and reviewing motion traces in several subjects^{106,107}; respiratory filtering is unsuitable for neonatal fMRI data due to the higher respiratory rate of neonates. Toddler (2-year and 3-year) fMRI data were censored based

on a threshold of $FD_{\text{fit}} > 0.2$ mm, using a filtered framewise displacement trace corrected for the effect of respiration (FIRMM filtered $FD^{108,109}$), with the additional restriction that only epochs of at least 3 consecutive frames $FD < 0.2$ mm were included.

In order to be included in the study, a minimum of 5 min (375 frames) of data retained after censoring was required, though 99% of scans across timepoints had >10 min of data retained after censoring ($M = 17.4$ min (1308 frames), range = 7.1–41.9 min). To account for any potential patterns of FC related to head motion or amount of data included in analyses, we calculated (i) the number of frames retained after censoring and (ii) the average FD across uncensored frames for each individual subject and included these values as subject-level covariates in all analyses. We additionally calculated (iii) the average FD across all frames for each individual subject, used as subject-level covariates in sensitivity analyses. Neither average uncensored FD nor total number of frames retained after censoring were related to prenatal disadvantage (uncensored FD : $r = 0.014$, $p = 0.77$; total number of frames: $r = 0.06$, $p = 0.22$).

fMRI data were aligned across subjects into the fs_LR32k surface space using spherical registration. Timecourses for surface data were smoothed with geodesic 2D Gaussian kernels ($\sigma = 2.25$ mm).

Network analysis

Residual mean BOLD time series from each participant at each timepoint were extracted from a 333-region cortical parcellation¹¹⁰. The functional connectivity matrix was represented as a graph or network¹¹¹. Network edges between nodes (brain regions) were represented by the Fisher z-transformed Pearson correlation between time courses from pairs of surface regions¹¹². Because there is not yet consensus on the spatial layout of neonatal functional networks^{105,113–118}, we assigned nodes to 13 large-scale functional systems (also sometimes called “networks”) based on the definitions of functional systems derived in healthy adults¹¹⁰.

Across the cortex, we calculated three summary measures of functional network segregation, which quantify the extent to which groups or subnetworks of nodes, or brain regions, display densely interconnected patterns of connectivity (see Fig. 1). System segregation, our measure of global segregation, quantifies the difference between mean within-system connectivity and mean between-system connectivity as a proportion of mean within-system connectivity^{4,9}, given an a priori partition of nodes into systems, in this case the 13 large-scale functional systems¹¹⁰. Modularity, quantified by the modularity quality index (Q), is a measure of meso-scale network segregation that estimates the extent to which the nodes of a network can be subdivided into groups or modules characterized by strong, dense intramodular connectivity and weak, sparse intermodular connectivity. Local segregation was measured using the clustering coefficient, which quantifies the amount of connectivity between a node and its strongest neighbors^{119–122}. A node has a high clustering coefficient when a high proportion of its neighbors are also strong neighbors of each other. Local segregation at the whole-brain level was calculated as the average of the clustering coefficient across all cortical regions. In later analyses of regional specificity, we examined the clustering coefficient of individual nodes or regions. We specifically chose measures of functional network architecture that were suitable for weighted, signed networks, when possible.

We also estimated a measure of functional network integration, the participation coefficient, which quantifies the diversity of a node's connections across systems^{42,123}. See Supplementary Methods for further details of network analysis and equations for measures of network segregation and integration.

Demographics and socioeconomic status

Mothers completed surveys in each trimester, at delivery, and during follow up visits every 4 months to assess social background, mental

health, and life experiences. Child race and ethnicity were obtained from the child's birth certificate, options included White, Black or African American, American Indian or Alaska Native, Asian Indian, Chinese, Filipino, Japanese, Korean, Vietnamese, Other Asian, Native Hawaiian, Guamanian or Chamorro, Samoan, Other Pacific Islander, or Other for race; ethnicity was assessed by whether the child was identified as Hispanic. Sex assigned at birth was obtained from child birth certificates. Prenatal disadvantage was assessed using a latent factor of socioeconomic disadvantage from a confirmatory factor analysis using MPlus software, which included measures of mother's income-to-needs ratio, educational attainment, area deprivation index, insurance status, and nutrition¹⁹. Maternal self-reported highest level of education and health insurance status were collected in trimester 1. Mothers reported household income and persons in the home to calculate INR in each trimester¹²⁴. Home addresses were collected at delivery to obtain Area Deprivation Index percentiles; the area deprivation index is a geocoding measure that ranks neighborhoods by socioeconomic disadvantage compared with the national average based on census block data, including factors for the domains of income, education, employment, and housing quality¹²⁵. Prior work in the eLABE cohort has shown that, while 26% of mothers changed addresses during pregnancy, there was no significant change in block groups during pregnancy¹²⁶, and we similarly find that there was not significant social mobility (change in ADI) during the study time period in our sample ($F_{s(\text{child age})} = 1.44, p = 0.19$). Maternal nutrition was assessed in the third trimester or at delivery using the Healthy Eating Index, a validated dietary assessment tool available through the National Institutes of Health used to measure diet quality based on U.S. Dietary Guidelines for Americans¹²⁷. Higher scores on the prenatal disadvantage factor are indicative of more disadvantage.

Data on demographic and socioeconomic indicators (education, household income, insurance status, ADI) were also collected during follow-up visits. Prenatal disadvantage was highly correlated with disadvantage at years 1–3 (r 's = 0.92–0.93, p 's < 1×10^{-16}). While we focus our analyses on the disadvantage factor assessed at birth, supplementary analyses investigate the contribution of disadvantage at later time points. Additionally, we examine the effect of using a composite variable of parental education and income to assess SES, rather than the disadvantage factor, for consistency with prior literature, in our sensitivity analyses.

Cognitive and language outcomes

The Bayley Scales of Infant and Toddler Development-Third Edition (Bayley-III) was used to assess cognitive, language, and motor abilities at both 2 and 3 years of age. Based on prior evidence that network segregation is associated with higher-order cognitive abilities in adults⁹, we specifically examined age-standardized cognitive and language composite scores ($M = 100, SD = 15$); the language composite consists of the Receptive Language and Expressive Language subscales. At the 2-year timepoint, $n = 90$ children had usable Bayley assessments and fMRI data (2 children with imaging data were excluded for low-quality or missing Bayley). At the three-year timepoint, $n = 66$ children had usable Bayley assessments and fMRI data (no children with imaging data were excluded for low-quality or missing Bayley).

Data analysis

Our analyses relating age and prenatal disadvantage to cortical functional network architecture were pre-registered at <https://aspredicted.org/eb5pd.pdf>. Any deviations from the original plan or additional exploratory analyses have been fully described below.

Statistical models

To flexibly model longitudinal linear and non-linear relationships between cortical functional network segregation and age, we implemented GAMMs (generalized additive mixed models) using the *mgcv*

package in R¹²⁸. GAMMs were fit with functional network segregation as the dependent variable, age as a smooth term, a random effect of participant, and biological sex assigned at birth, in-scanner motion (average framewise displacement), number of frames of fMRI retained after censoring, and average functional network weight (average network connectivity) as linear covariates. Each GAMM estimates a smooth function (the model age fit, generated from a linear combination of weighted basis functions) that describes the relationship between functional network segregation and age, thus modeling the developmental trajectory of network segregation. Four basis functions were specified as the maximum flexibility afforded to age splines in all models ($k = 4$). Models were fit using thin plate regression splines as the smooth term basis set and the restricted maximal likelihood approach for smoothing parameter selection. Average network weight was included to control for global differences in connectivity strength^{129–131}. Random effects included a random intercept per participant. To test for windows of significant change across the age range, we calculated the first derivative of the smooth function of age from the GAMM model using finite differences, and then generated a simultaneous 95% confidence interval of the derivative¹³² using the *gratia* package in R. The first derivative of this smooth function represents the rate of change in network segregation at a given developmental time point. Intervals of significant age-related change were identified as areas where the simultaneous confidence interval of the derivative does not include zero. Multiple comparisons correction was applied across models of developmental changes in cortical functional network segregation using FDR correction¹³³.

To examine associations between prenatal disadvantage and age-related increases in functional network segregation, we allowed the smoothed age effect in the GAMM to interact with prenatal disadvantage; predictors thus included an age-by-disadvantage interaction term, a smooth term for age, and covariates including sex, in-scanner motion, number of frames of fMRI, and average network weight. We compared two interaction models: a simpler varying coefficient (linear-nonlinear) model that allows the smooth term for age to vary as a linear function of prenatal disadvantage, and a more complex non-linear interaction (bivariate smooth) model that allows the smooth term for age to vary as a fully non-linear function of prenatal disadvantage. We compared models using Bayesian information criterion (BIC), and evaluated the significance of the interaction term for the selected model. All models were best fit using the simpler varying coefficient (linear-nonlinear) model that allows the linear association between prenatal disadvantage and network segregation to vary as a smooth function of age. Interaction p -values were confirmed using a parametric bootstrap likelihood ratio test (*pbkrtest* package in R) for significance estimation in the mixed model context. Multiple comparisons correction was applied across models of age-by-disadvantage associations with cortical functional network segregation using FDR correction. While prenatal disadvantage was modeled continuously, for visualization purposes in plots we show trajectories from the highest and lowest deciles.

To evaluate the scale at which prenatal disadvantage is associated with measures of functional network segregation, we fit models for each of our measures of local, meso-scale, and global segregation in turn, controlling for each of the other measures of segregation. For example, we first fit a GAMM for the age-by-disadvantage effect on system segregation while including modularity as a fixed effect, then fit a GAMM for age-by-disadvantage effects on system segregation while including the clustering coefficient as a fixed effect.

To characterize regional specificity of prenatal disadvantage associations with maturational changes in local segregation, we fit region-specific GAMMs with the same interaction structure and covariates as the whole-brain models. Models were fit separately for each parcellated cortical region. For each regional GAMM, the significance of the age-by-disadvantage interaction term was assessed in a fixed

degree-of-freedom context to ensure stable and accurate estimation. We corrected p -values across all region-wise GAMMs using FDR correction and set statistical significance at $p_{\text{FDR}} < 0.05$. To establish the overall magnitude of the moderating effect of prenatal disadvantage on age-associated increases in local segregation, which we refer to throughout as a region's overall age-by-disadvantage effect magnitude, we used the F -statistic for the age-by-disadvantage interaction effect. To evaluate the age-by-disadvantage effect across functional systems, we used the effect magnitude at each parcel within each system. A Kruskal–Wallis test was used to compare the magnitude of the age-by-disadvantage effects across functional systems.

Moderating effects of prenatal disadvantage on associations between age and language composite scores were also modeled with GAMMs; we allowed the smoothed age effect in the GAMM to interact with disadvantage, using the same model comparison framework as above. We tested a varying-coefficient (linear-nonlinear) model and a more complex fully non-linear interaction (bivariate smooth) model, comparing models using Bayesian information criterion (BIC), and evaluated the significance of the interaction term for the selected model; the bivariate smooth model fit the language composite best, while the linear-nonlinear model fit the cognitive composite best. Note that as these the composite scores are standardized for age, the smoothed effect of age in this model solely accounts for variation over time in language scores relative to age norms.

When examining relationships between local cortical network segregation and language outcomes at the 2-year and 3-year timepoints, due to the smaller number of datapoints available, we used linear models (results are qualitatively unchanged when using GAMs). We estimated associations between local segregation and Bayley language scaled scores, controlling for biological sex assigned at birth, in-scanner motion (average framewise displacement), number of frames of fMRI retained after censoring, and average functional network weight. Multiple comparisons correction was applied across each set of two models using FDR correction.

Comparison of cortical maps

A previously derived axis of sensorimotor-association cortical organization⁸ was retrieved from https://github.com/PennLINC/S-A_ArchetypalAxis. To quantify the association between S-A axis ranks and observed environmental effects on developmental increases in local segregation, we used Spearman's rank correlations and tested for statistical significance using spin-based spatial permutation tests^{134,135}, which account for spatial covariance structure common in neuroimaging data. We generated a null distribution based on 10,000 spherical rotations, and compared the observed value to the null.

Deviations from pre-registration

We did not conduct some analyses in the pre-registration that were deemed potential exploratory analyses and turned out to be unhelpful in elucidating the effects we found. Specifically, as the primary driver of the age-by-disadvantage effect was found to be on local segregation (the clustering coefficient) and alterations in local topology, we did not examine age-by-disadvantage effects on within- and between-system connectivity; this analysis would have been informative for probing age-by-disadvantage effects on system segregation. As our measure of local segregation, the clustering coefficient, does not rely on an a priori assignment of regions to functional systems, we deemed an analysis of functional-system-level connectivity unhelpful in investigating the effects we found here. Also, in a follow-up analysis we had planned to examine the effect of including only participants whose disadvantage factor score did not change by $>1SD$ between timepoints. However, as upon investigation there was little change in direct indicators of disadvantage during the study period (see Supplementary Fig. 3),

and the composition of the disadvantage factor score changed from the birth to toddler timepoints (prenatal Healthy Eating Index was removed from the factor score), we decided not to pursue this analysis.

Additionally, we include here follow-up analyses that were not part of our pre-registration to probe the contributors and potential behavioral associations of the moderating associations of prenatal disadvantage with cortical functional network development trajectories that we found in the pre-registered analyses. Specifically, we examined a) which scale of segregation was the fundamental driver of age-by-disadvantage effects on cortical network segregation, b) regional variation in age-by-disadvantage effects on local segregation, and c) associations between local segregation and language and cognitive outcomes. These analyses were not pre-registered and should be considered exploratory in nature.

Finally, we initially planned to rerun any GAMMs with estimated degrees of freedom (EDF) of the age smooth <2 as linear mixed effects models, but upon visual inspection of developmental trajectories of cortical network segregation, non-linear models of age seemed appropriate even for those measures with age EDFs slightly under 2. As GAMMs can model both linear and non-linear relationships, in the case that there is no non-linear relationship between age and an outcome measure, the smooth term for age will be penalized down to a linear term. Thus, for ease of comparison and to avoid switching modeling approaches, we have instead used GAMMs for all models in the included analyses.

Citation diversity statement

Recent work in several fields of science has identified a bias in citation practices such that papers from women and other under-represented scholars are undercited relative to the number of such papers in the field^{136–142}. We used prior methods^{140,143} to measure that our references contain 20.69% woman(first)/woman(last), 21.12% man/woman, 26.87% woman/man, and 31.31% man/man authors. This method is limited in that (a) names, pronouns, and social media profiles used to construct the databases may not, in every case, be indicative of gender identity and (b) it cannot account for intersex, non-binary, or transgender people. We used additional methods^{144,145} to measure that our references contain 11.82% author of color (first)/author of color(last), 14.11% white author/author of color, 21.51% author of color/white author, and 52.56% white author/white author. This method is limited in that (a) names, Census entries, and Wikipedia profiles used to predict racial and ethnic categories may not be indicative of racial or ethnic identity, and (b) it cannot account for Indigenous and mixed-race authors, or those who may face differential biases due to the ambiguous racialization or ethnicization of their names. We look forward to future work that could help us to better understand how to support equitable practices in science.

Reporting summary

Further information on research design is available in the Nature Portfolio Reporting Summary linked to this article.

Data availability

The derived neural and behavioral data (processed and aggregated final data in CSV form) that can be used to replicate the findings have been deposited in Github (<https://zenodo.org/doi/10.5281/zenodo.12785442>). The deidentified data (metric outputs from imaging data after preprocessing and labeled spreadsheets) from the eLABLE sample will be deposited into the NIMH Data Archive repository upon conclusion of the longitudinal portion of the study, as per NIH rules and regulations. Study analyses additionally made use of publicly available cortical atlases, including the Gordon 333-region parcellation (<https://balsa.wustl.edu/2Vm69>) and the sensorimotor-association axis (https://pennlinc.github.io/S-A_ArchetypalAxis/).

Code availability

All statistical analyses were conducted in R4.1.2 (<https://www.r-project.org/>) and MATLAB R2021b. Functions from the Brain Connectivity Toolbox¹²³ were used to calculate measures of network segregation and integration. Freely available MATLAB code from https://github.com/mychan24/system_matrix_tools was used to calculate system segregation. Surfaces and regional effects were shown on cortical surfaces generated by MCRIB using the *cifti* and *ciftiTools* packages¹⁴⁶ and Connectome Workbench 7.2. Code for all analyses presented here is publicly available at https://github.com/utooley/Tooley2023_prenatal_env_cortical_network_dev, and has been deposited into Zenodo¹⁴⁷.

References

- Zhao, T., Xu, Y. & He, Y. Graph theoretical modeling of baby brain networks. *NeuroImage* <https://doi.org/10.1016/j.neuroimage.2018.06.038> (2018).
- Wen, X. et al. First-year development of modules and hubs in infant brain functional networks. *NeuroImage* **185**, 222–235 (2019).
- Grayson, D. S. & Fair, D. A. Development of large-scale functional networks from birth to adulthood: a guide to the neuroimaging literature. *NeuroImage* **160**, 15–31 (2017).
- Wig, G. S. Segregated systems of human brain networks. *Trends Cogn. Sci.* **21**, 981–996 (2017).
- Gao, W. et al. The Synchronization within and Interaction between the Default and Dorsal Attention Networks in Early Infancy. *Cereb. Cortex* **23**, 594–603 (2013).
- Gu, S. et al. Emergence of system roles in normative neurodevelopment. *Proc. Natl Acad. Sci. USA* **112**, 13681–13686 (2015).
- Tooley, U. A. et al. The age of reason: functional brain network development during childhood. *J. Neurosci.* **42**, 8237–8251 (2022).
- Sydnor, V. J. et al. Neurodevelopment of the association cortices: patterns, mechanisms, and implications for psychopathology. *Neuron* **109**, 2820–2846 (2021).
- Chan, M. Y., Park, D. C., Savalia, N. K., Petersen, S. E. & Wig, G. S. Decreased segregation of brain systems across the healthy adult lifespan. *Proc. Natl Acad. Sci. USA* **111**, E4997–E5006 (2014).
- Cohen, J. R. & D'Esposito, M. The segregation and integration of distinct brain networks and their relationship to cognition. *J. Neurosci.* **36**, 12083–12094 (2016).
- Zhang, H. & Diaz, M. T. Resting state network segregation modulates age-related differences in language production. *Neurobiol. Lang.* 1–22 https://doi.org/10.1162/nol_a_00106 (2023).
- Nashiro, K., Sakaki, M., Braskie, M. N. & Mather, M. Resting-state networks associated with cognitive processing show more age-related decline than those associated with emotional processing. *Neurobiol. Aging* **54**, 152–162 (2017).
- Cohen, S., Janicki-Deverts, D., Chen, E. & Matthews, K. A. Childhood socioeconomic status and adult health. *Ann. N. Y. Acad. Sci.* **1186**, 37–55 (2010).
- Bundy, J. D. et al. Social determinants of health and premature death among adults in the USA from 1999 to 2018: a national cohort study. *Lancet Public Health* **8**, e422–e431 (2023).
- Kaplan, G. A. et al. Childhood socioeconomic position and cognitive function in adulthood. *Int. J. Epidemiol.* **30**, 256–263 (2001).
- Evans, G. W. & Cassells, R. C. Childhood poverty, cumulative risk exposure, and mental health in emerging adults. *Clin. Psychol. Sci. J. Assoc. Psychol. Sci.* **2**, 287–296 (2014).
- Farah, M. J. The neuroscience of socioeconomic status: correlates, causes, and consequences. *Neuron* **96**, 56–71 (2017).
- Kachmar, A. G., Connolly, C. A., Wolf, S. & Curley, M. A. Q. Socioeconomic status in pediatric health research: a scoping review. *J. Pediatr.* **213**, 163–170 (2019).
- Luby, J. L. et al. Social disadvantage during pregnancy: effects on gestational age and birthweight. *J. Perinatol.* **43**, 477–483 (2023).
- Tooley, U. A. et al. Associations between neighborhood SES and functional brain network development. *Cereb. Cortex* **30**, 1–19 (2020).
- Gellci, K. et al. Community and household-level socioeconomic disadvantage and functional organization of the salience and emotion network in children and adolescents. *NeuroImage* **184**, 729–740 (2019).
- Tooley, U. A., Bassett, D. S. & Mackey, A. P. Environmental influences on the pace of brain development. *Nat. Rev. Neurosci.* **22**, 372–384 (2021).
- Ramphal, B. et al. Brain connectivity and socioeconomic status at birth and externalizing symptoms at age 2 years. *Dev. Cogn. Neurosci.* 100811 <https://doi.org/10.1016/j.dcn.2020.100811> (2020).
- Gao, W. et al. Functional network development during the first year: relative sequence and socioeconomic correlations. *Cereb. Cortex* **25**, 2919–2928 (2015).
- Kaufmann, T. et al. Common brain disorders are associated with heritable patterns of apparent aging of the brain. *Nat. Neurosci.* **22**, 1617–1623 (2019).
- Karolinska Schizophrenia Project (KaSP). et al. Common brain disorders are associated with heritable patterns of apparent aging of the brain. *Nat. Neurosci.* **22**, 1617–1623 (2019).
- Shaw, P., Gogtay, N. & Rapoport, J. Childhood psychiatric disorders as anomalies in neurodevelopmental trajectories. *Hum. Brain Mapp.* **31**, 917–925 (2010).
- Mendle, J., Harden, K. P., Brooks-Gunn, J. & Gruber, J. A. Development's tortoise and hare: pubertal timing, pubertal tempo, and depressive symptoms in boys and girls. *Dev. Psychol.* **46**, 1341–1353 (2010).
- Colich, N. L. et al. Earlier age at menarche as a transdiagnostic mechanism linking childhood trauma with multiple forms of psychopathology in adolescent girls. *Psychol. Med.* **50**, 1090–1098 (2020).
- Deardorff, J. et al. Girls' pubertal timing and tempo and mental health: a longitudinal examination in an ethnically diverse sample. *J. Adolesc. Health* **68**, 1197–1203 (2021).
- Hensch, T. K. Critical period plasticity in local cortical circuits. *Nat. Rev. Neurosci.* **6**, 877–888 (2005).
- Werker, J. F. & Hensch, T. K. Critical periods in speech perception: new directions. *Annu. Rev. Psychol.* **66**, 173–196 (2015).
- Ellis, B. J., Sheridan, M. A., Belsky, J. & McLaughlin, K. A. Why and how does early adversity influence development? Toward an integrated model of dimensions of environmental experience. *Dev. Psychopathol.* **34**, 447–471 (2022).
- Belsky, J., Schlomer, G. L. & Ellis, B. J. Beyond cumulative risk: distinguishing harshness and unpredictability as determinants of parenting and early life history strategy. *Dev. Psychol.* **48**, 662–673 (2012).
- Frankenhuis, W. E. & Amir, D. What is the expected human childhood? Insights from evolutionary anthropology. *Dev. Psychopathol.* **34**, 473–497 (2022).
- Roubinov, D., Meaney, M. J. & Boyce, W. T. Change of pace: How developmental tempo varies to accommodate failed provision of early needs. *Neurosci. Biobehav. Rev.* <https://doi.org/10.1016/j.neubiorev.2021.09.031> (2021).
- Rakesh, D., Whittle, S., Sheridan, M. A. & McLaughlin, K. A. Childhood socioeconomic status and the pace of structural neurodevelopment: accelerated, delayed, or simply different? *Trends Cogn. Sci.* <https://doi.org/10.1016/j.tics.2023.03.011> (2023).
- Lean, R. E. et al. Prenatal exposure to maternal social disadvantage and psychosocial stress and neonatal white matter connectivity at birth. *Proc. Natl. Acad. Sci. USA* **119**, e2204135119 (2022).
- Triplet, R. L. et al. Association of prenatal exposure to early-life adversity with neonatal brain volumes at birth. *JAMA Netw. Open* **5**, e227045 (2022).

40. Herzberg, M. P. et al. Maternal prenatal social disadvantage and neonatal functional connectivity: Associations with psychopathology symptoms at age 12 months. *Dev. Psychol.* No Pagination Specified-No Pagination Specified <https://doi.org/10.1037/dev0001708> (2024).
41. Bassett, D. S. & Bullmore, E. T. Small-world brain networks revisited. *Neuroscientist* **23**, 499–516 (2017).
42. Guimerà, R. & Nunes Amaral, L. A. Functional cartography of complex metabolic networks. *Nature* **433**, 895–900 (2005).
43. Marek, S., Hwang, K., Foran, W., Hallquist, M. N. & Luna, B. The contribution of network organization and integration to the development of cognitive control. *PLoS Biol.* **13**, e1002328 (2015).
44. Sanders, A. F. P. et al. Age-related differences in resting-state functional connectivity from childhood to adolescence. *Cereb. Cortex* bhad011 <https://doi.org/10.1093/cercor/bhad011> (2023).
45. Sydnor, V. J. et al. Intrinsic activity development unfolds along a sensorimotor-association cortical axis in youth. *Nat Neurosci.* **26**, 638–649 (2023).
46. Tanti, A. et al. Region-dependent and stage-specific effects of stress, environmental enrichment, and antidepressant treatment on hippocampal neurogenesis. *Hippocampus* **23**, 797–811 (2013).
47. Bath, K. G., Manzano-Nieves, G. & Goodwill, H. Early life stress accelerates behavioral and neural maturation of the hippocampus in male mice. *Horm. Behav.* **82**, 64–71 (2016).
48. Manzano Nieves, G., Bravo, M., Baskoylu, S. & Bath, K. G. Early life adversity decreases pre-adolescent fear expression by accelerating amygdala PV cell development. *eLife* **9**, e55263 (2020).
49. Goodwill, H. L. et al. Early life stress drives sex-selective impairment in reversal learning by affecting parvalbumin interneurons in orbitofrontal cortex of mice. *Cell Rep.* **25**, 2299–2307.e4 (2018).
50. Lebel, C., Treit, S. & Beaulieu, C. A review of diffusion MRI of typical white matter development from early childhood to young adulthood. *NMR Biomed.* **32**, e3778 (2019).
51. Lebel, C. & Deoni, S. The development of brain white matter microstructure. *NeuroImage* **182**, 207–218 (2018).
52. Chan, M. Y. et al. Long-term prognosis and educational determinants of brain network decline in older adult individuals. *Nat. Aging* **1**, 1053–1067 (2021).
53. Chan, M. Y. et al. Socioeconomic status moderates age-related differences in the brain's functional network organization and anatomy across the adult lifespan. *Proc. Natl. Acad. Sci. USA* **115**, E5144–E5153 (2018).
54. Corbetta, M. & Shulman, G. L. Control of goal-directed and stimulus-driven attention in the brain. *Nat. Rev. Neurosci.* **3**, 201–215 (2002).
55. Greenberg, A. S. et al. Visuotopic cortical connectivity underlying attention revealed with white-matter tractography. *J. Neurosci. J. Soc. Neurosci.* **32**, 2773–2782 (2012).
56. Dong, H.-M., Margulies, D. S., Zuo, X.-N. & Holmes, A. J. Shifting gradients of macroscale cortical organization mark the transition from childhood to adolescence. *Proc. Natl. Acad. Sci. USA* **118**, e2024448118 (2021).
57. Rosen, M. L., Amso, D. & McLaughlin, K. A. The role of the visual association cortex in scaffolding prefrontal cortex development: a novel mechanism linking socioeconomic status and executive function. *Dev. Cogn. Neurosci.* 100699 <https://doi.org/10.1016/j.dcn.2019.100699> (2019).
58. Rakesh, D., Seguin, C., Zalesky, A., Cropley, V. & Whittle, S. Associations between neighborhood disadvantage, resting-state functional connectivity, and behavior in the adolescent brain cognitive development study: the moderating role of positive family and school environments. *Biol. Psychiatry Cogn. Neurosci. Neuroimaging* **6**, 877–886 (2021).
59. Rakesh, D., Zalesky, A. & Whittle, S. Similar but distinct—effects of different socioeconomic indicators on resting state functional connectivity: findings from the Adolescent Brain Cognitive Development (ABCD) Study®. *Dev. Cogn. Neurosci.* **51**, 101005 (2021).
60. Sripada, C. et al. Socioeconomic resources are associated with distributed alterations of the brain's intrinsic functional architecture in youth. *Dev. Cogn. Neurosci.* **58**, 101164 (2022).
61. Modabbernia, A., Janiri, D., Doucet, G. E., Reichenberg, A. & Frangou, S. Multivariate patterns of brain-behavior-environment associations in the adolescent brain and cognitive development study. *Biol. Psychiatry* **89**, 510–520 (2021).
62. Song, X. et al. Long-term decline in intergenerational mobility in the United States since the 1850s. *Proc. Natl. Acad. Sci. USA* **117**, 251–258 (2020).
63. Chetty, R. et al. The fading American dream: trends in absolute income mobility since 1940. *Science* **356**, 398–406 (2017).
64. Mueller, S. et al. Individual variability in functional connectivity architecture of the human brain. *Neuron* **77**, 586–595 (2013).
65. Stoecklein, S. et al. Variable functional connectivity architecture of the preterm human brain: Impact of developmental cortical expansion and maturation. *Proc. Natl. Acad. Sci. USA* **117**, 1201–1206 (2020).
66. Bruchhage, M. M. K., Ngo, G.-C., Schneider, N., D'Sa, V. & Deoni, S. C. L. Functional connectivity correlates of infant and early childhood cognitive development. *Brain Struct. Funct.* **225**, 669–681 (2020).
67. King, L. S., Camacho, M. C., Montez, D. F., Humphreys, K. L. & Gotlib, I. H. Naturalistic language input is associated with resting-state functional connectivity in infancy. *J. Neurosci.* **41**, 424–434 (2021).
68. Yue, Q. et al. Brain modularity mediates the relation between task complexity and performance. *J. Cogn. Neurosci.* **29**, 1532–1546 (2017).
69. Sheridan, M. A. & McLaughlin, K. A. Dimensions of early experience and neural development: deprivation and threat. *Trends Cogn. Sci.* **18**, 580–585 (2014).
70. McLaughlin, K. A., Sheridan, M. A. & Lambert, H. K. Childhood adversity and neural development: deprivation and threat as distinct dimensions of early experience. *Neurosci. Biobehav. Rev.* **47**, 578–591 (2014).
71. Bradley, R. H., Corwyn, R. F., McAdoo, H. P. & Coll, C. G. The home environments of children in the United States part I: variations by age, ethnicity, and poverty status. *Child Dev.* **72**, 1844–1867 (2001).
72. Favuzzi, E. et al. Activity-dependent gating of parvalbumin interneuron function by the perineuronal net protein brevicain. *Neuron* **95**, 639–655.e10 (2017).
73. Duffy, S. N. Environmental enrichment modifies the PKA-dependence of hippocampal LTP and improves hippocampus-dependent memory. *Learn. Mem.* **8**, 26–34 (2001).
74. Bao, S., Chan, V. T. & Merzenich, M. M. Cortical remodelling induced by activity of ventral tegmental dopamine neurons. *Nature* **412**, 79–83 (2001).
75. Vetencourt, J. F. M. et al. The antidepressant fluoxetine restores plasticity in the adult visual cortex. *Science* **320**, 385–388 (2008).
76. Bear, M. F. & Singer, W. Modulation of visual cortical plasticity by acetylcholine and noradrenaline. *Nature* **320**, 172–176 (1986).
77. Gee, D. G. et al. Early developmental emergence of human amygdala–prefrontal connectivity after maternal deprivation. *Proc. Natl. Acad. Sci. USA* **110**, 15638–15643 (2013).
78. McEwen, B. S. Stress, adaptation, and disease. Allostasis and allostatic load. *Ann. N. Y. Acad. Sci.* **840**, 33–44 (1998).
79. Snell-Rood, E. & Snell-Rood, C. The developmental support hypothesis: adaptive plasticity in neural development in response to cues of social support. *Philos. Trans. R. Soc. B Biol. Sci.* **375**, 20190491 (2020).
80. Baum, A., Garofalo, J. P. & Yali, A. M. Socioeconomic status and chronic stress: Does stress account for SES effects on health? *Ann. N. Y. Acad. Sci.* **896**, 131–144 (1999).

81. Bassett, D. S., Yang, M., Wymbs, N. F. & Grafton, S. T. Learning-induced autonomy of sensorimotor systems. *Nat. Neurosci.* **18**, 744–751 (2015).
82. Rueda, M. R., Rothbart, M. K., McCandliss, B. D., Saccomanno, L. & Posner, M. I. Training, maturation, and genetic influences on the development of executive attention. *Proc. Natl. Acad. Sci. USA* **102**, 14931–14936 (2005).
83. Romeo, R. R. et al. Beyond the “30 million word gap:” Children’s conversational exposure is associated with language-related brain function. *Psychol. Sci.* **29**, 700–710 (2018).
84. Herringa, R. J. et al. Enhanced prefrontal-amygdala connectivity following childhood adversity as a protective mechanism against internalizing in adolescence. *Biol. Psychiatry Cogn. Neurosci. Neuroimaging* **1**, 326–334 (2016).
85. Gopnik, A. Childhood as a solution to explore–exploit tensions. *Philos. Trans. R. Soc. B Biol. Sci.* **375**, 20190502 (2020).
86. Frankenhuis, W. E. & Walasek, N. Modeling the evolution of sensitive periods. *Dev. Cogn. Neurosci.* **41**, 100715 (2020).
87. Panchanathan, K. & Frankenhuis, W. E. The evolution of sensitive periods in a model of incremental development. *Proc. R. Soc. B Biol. Sci.* **283**, 20152439 (2016).
88. Frankenhuis, W. E. & Panchanathan, K. Individual differences in developmental plasticity may result from stochastic sampling. *Perspect. Psychol. Sci.* **6**, 336–347 (2011).
89. Chang, E. F. & Merzenich, M. M. Environmental noise retards auditory cortical development. *Science* **300**, 498–502 (2003).
90. Erchova, I., Vasalaukaite, A., Longo, V. & Sengpiel, F. Enhancement of visual cortex plasticity by dark exposure. *Philos. Trans. R. Soc. B Biol. Sci.* **372**, 20160159 (2017).
91. Dumornay, N. M., Lebois, L. A. M., Ressler, K. J. & Harnett, N. G. Racial disparities in adversity during childhood and the false appearance of race-related differences in brain structure. *Am. J. Psychiatry* **180**, 127–138 (2023).
92. Barch, D. M. & Luby, J. L. Understanding social determinants of brain health during development. *Am. J. Psychiatry* **180**, 108–110 (2023).
93. Callaghan, B. L. & Tottenham, N. The stress acceleration hypothesis: effects of early-life adversity on emotion circuits and behavior. *Curr. Opin. Behav. Sci.* **7**, 76–81 (2016).
94. Short, A. K. & Baram, T. Z. Early-life adversity and neurological disease: age-old questions and novel answers. *Nat. Rev. Neurol.* **1–13** <https://doi.org/10.1038/s41582-019-0246-5> (2019).
95. Myers, M. J. et al. Functional parcellation of the neonatal cortical surface. *Cereb. Cortex* **34**, bhac047 (2024).
96. Wang, F. et al. Fine-grained functional parcellation maps of the infant cerebral cortex. *eLife* **12**, e75401 (2023).
97. Volkow, N. D., Gordon, J. A. & Freund, M. P. The Healthy Brain and Child Development Study—Shedding Light on Opioid Exposure, COVID-19, and Health Disparities. *JAMA Psychiatry* <https://doi.org/10.1001/jamapsychiatry.2020.3803> (2020).
98. Averett, S. & Wang, Y. Effects of higher EITC payments on children’s health, quality of home environment, and noncognitive skills. *Public Financ. Rev.* **46**, 519–557 (2018).
99. Bitler, M., Hoynes, H. & Kuka, E. Child poverty, the great recession, and the social safety net in the United States. *J. Policy Anal. Manag.* **36**, 358–389 (2017).
100. Sperber, J. F. et al. Unconditional cash transfers and maternal assessments of children’s health, nutrition, and sleep: a randomized clinical trial. *JAMA Netw. Open* **6**, e2335237 (2023).
101. Baltagi, B. H. & Yen, Y.-F. Welfare reform and children’s health. *Health Econ.* **25**, 277–291 (2016).
102. Stout, M. J. et al. A multidisciplinary prematurity research cohort study. *PLoS One* **17**, e0272155 (2022).
103. Dosenbach, N. U. F. et al. Real-time motion analytics during brain MRI improve data quality and reduce costs. *NeuroImage* **161**, 80–93 (2017).
104. Badke & D’Andrea, C. et al. Real-time motion monitoring improves functional MRI data quality in infants. *Dev. Cogn. Neurosci.* **55**, 101116 (2022).
105. Smyser, C. D. et al. Longitudinal analysis of neural network development in preterm infants. *Cereb. Cortex* **20**, 2852–2862 (2010).
106. Power, J. D., Barnes, K. A., Snyder, A. Z., Schlaggar, B. L. & Petersen, S. E. Spurious but systematic correlations in functional connectivity MRI networks arise from subject motion. *NeuroImage* **59**, 2142–2154 (2012).
107. Power, J. D. et al. Methods to detect, characterize, and remove motion artifact in resting state fMRI. *NeuroImage* **84**, 320–341 (2014).
108. Kaplan, S. et al. Filtering respiratory motion artifact from resting state fMRI data in infant and toddler populations. *NeuroImage* **247**, 118838 (2022).
109. Fair, D. A. et al. Correction of respiratory artifacts in MRI head motion estimates. *NeuroImage* **208**, 116400 (2020).
110. Gordon, E. M. et al. Generation and evaluation of a cortical area parcellation from resting-state correlations. *Cereb. Cortex N. Y. NY* **26**, 288–303 (2016).
111. Bassett, D. S., Zurn, P. & Gold, J. I. On the nature and use of models in network neuroscience. *Nat. Rev. Neurosci.* **19**, 566 (2018).
112. Zalesky, A., Fornito, A. & Bullmore, E. On the use of correlation as a measure of network connectivity. *NeuroImage* **60**, 2096–2106 (2012).
113. Lin, W. et al. Functional connectivity MR imaging reveals cortical functional connectivity in the developing brain. *AJNR Am. J. Neuroradiol.* **29**, 1883–1889 (2008).
114. Gao, W. et al. Evidence on the emergence of the brain’s default network from 2-week-old to 2-year-old healthy pediatric subjects. *Proc. Natl. Acad. Sci. USA* **106**, 6790–6795 (2009).
115. Doria, V. et al. Emergence of resting state networks in the preterm human brain. *Proc. Natl. Acad. Sci. USA* **107**, 20015–20020 (2010).
116. Gao, W., Alcauter, S., Smith, J. K., Gilmore, J. & Lin, W. Development of human brain cortical network architecture during infancy. *Brain Struct. Funct.* **220**, 1173–1186 (2015).
117. Eyre, M. et al. The Developing Human Connectome Project: typical and disrupted perinatal functional connectivity. *Brain* **144**, 2199–2213 (2021).
118. Sylvester, C. M. et al. Network-specific selectivity of functional connections in the neonatal brain. *Cereb. Cortex* bhac202 <https://doi.org/10.1093/cercor/bhac202> (2022).
119. Achard, S., Salvador, R., Whitcher, B., Suckling, J. & Bullmore, E. A resilient, low-frequency, small-world human brain functional network with highly connected association cortical hubs. *J. Neurosci.* **26**, 63–72 (2006).
120. Bartolomei, F. et al. Disturbed functional connectivity in brain tumour patients: evaluation by graph analysis of synchronization matrices. *Clin. Neurophysiol.* **117**, 2039–2049 (2006).
121. Bassett, D. S., Meyer-Lindenberg, A., Achard, S., Duke, T. & Bullmore, E. Adaptive reconfiguration of fractal small-world human brain functional networks. *Proc. Natl. Acad. Sci. USA* **103**, 19518–19523 (2006).
122. Xu, T. et al. Network analysis of functional brain connectivity in borderline personality disorder using resting-state fMRI. *NeuroImage Clin.* **11**, 302–315 (2016).
123. Rubinov, M. & Sporns, O. Complex network measures of brain connectivity: uses and interpretations. *NeuroImage* **52**, 1059–1069 (2010).
124. Office of the Assistant Secretary for Planning and Evaluation, Poverty Guidelines. U.S. Federal Poverty Guidelines Used to Determine Financial Eligibility for Certain Programs. *ASPE* <https://aspe.hhs.gov/topics/poverty-economic-mobility/poverty-guidelines>.
125. Kind, A. J. H. & Buckingham, W. R. Making neighborhood-disadvantage metrics accessible—the neighborhood atlas. *N. Engl. J. Med.* **378**, 2456–2458 (2018).

126. Brady, R. G. et al. The effects of prenatal exposure to neighborhood crime on neonatal functional connectivity. *Biol. Psychiatry* **92**, 139–148 (2022).
127. Krebs-Smith, S. M. et al. Update of the Healthy Eating Index: HEI-2015. *J. Acad. Nutr. Diet.* **118**, 1591–1602 (2018).
128. Wood, S. N. Stable and efficient multiple smoothing parameter estimation for generalized additive models. *J. Am. Stat. Assoc.* **99**, 673–686 (2004).
129. Van Wijk, B. C. M., Stam, C. J. & Daffertshofer, A. Comparing brain networks of different size and connectivity density using graph theory. *PLoS One* **5**, e13701 (2010).
130. Ginestet, C. E., Nichols, T. E., Bullmore, E. T. & Simmons, A. Brain network analysis: separating cost from topology using cost-integration. *PLoS One* **6**, e21570 (2011).
131. Yan, C.-G., Craddock, R. C., Zuo, X.-N., Zang, Y.-F. & Milham, M. P. Standardizing the intrinsic brain: towards robust measurement of inter-individual variation in 1000 functional connectomes. *NeuroImage* **80**, 246–262 (2013).
132. Simpson, G. L. Modelling palaeoecological time series using generalised additive models. *Front. Ecol. Evol.* **6**, 149 (2018).
133. Benjamini, Y. & Hochberg, Y. Controlling the false discovery rate: a practical and powerful approach to multiple testing. *J. R. Stat. Soc. B Methodol.* **57**, 289–300 (1995).
134. Alexander-Bloch, A. F. et al. On testing for spatial correspondence between maps of human brain structure and function. *NeuroImage* **178**, 540–551 (2018).
135. Váša, F. et al. Adolescent tuning of association cortex in human structural brain networks. *Cereb. Cortex N. Y. N. 1991* **28**, 281–294 (2018).
136. Mitchell, S. M., Lange, S. & Brus, H. Gendered citation patterns in international relations journals. *Int. Stud. Perspect.* **14**, 485–492 (2013).
137. Dion, M. L., Sumner, J. L. & Mitchell, S. M. Gendered citation patterns across political science and social science methodology fields. *Polit. Anal.* **26**, 312–327 (2018).
138. Caplar, N., Tacchella, S. & Birrer, S. Quantitative evaluation of gender bias in astronomical publications from citation counts. *Nat. Astron.* **1**, 1–5 (2017).
139. Maliniak, D., Powers, R. & Walter, B. F. The gender citation gap in international relations. *Int. Organ.* **67**, 889–922 (2013).
140. Dworkin, J. D. et al. The extent and drivers of gender imbalance in neuroscience reference lists. *Nat. Neurosci.* **23**, 918–926 (2020).
141. Wang, X. et al. Gendered citation practices in the field of communication. *Ann. Int. Commun. Assoc.* **45**, 134–153 (2021).
142. Chatterjee, P. & Werner, R. M. Gender disparity in citations in high-impact journal articles. *JAMA Netw. Open* **4**, e2114509 (2021).
143. Zhou, D. et al. Gender Diversity Statement and Code Notebook v1.0. <https://doi.org/10.5281/zenodo.3672110> (2020).
144. Ambekar, A., Ward, C., Mohammed, J., Male, S. & Skiena, S. Name-ethnicity classification from open sources. In *Proceedings of the 15th ACM SIGKDD International Conference on Knowledge Discovery and Data Mining* 49–58 (2009).
145. Sood, G. & Laohaprapanon, S. Predicting race and ethnicity from the sequence of characters in a name. *ArXiv Prepr. ArXiv180502109* (2018).
146. Pham, D., Muschelli, J. & Mejia, A. ciftiTools: a package for reading, writing, visualizing and manipulating CIFTI files in. *R. NeuroImage* **250**, 118877 (2022).
147. Tooley, U. Prenatal environment is associated with the pace of cortical network development over the first three years of life. *Zenodo*. <https://doi.org/10.5281/zenodo.12785442> (2024).
- thank the past and current team members of the March of Dimes Prematurity Research Center at Washington University in St Louis, the Early Emotional Development Program at Washington University in St Louis, and the Washington University Neonatal Development Research Group. This research was supported by the National Institute of Health (grant nos. R01 MH121877 to J.L.L. and C.E.R., R01 DAO46224 to C.E.R., R01 MH113570 to C.D.S. and C.E.R., R01 MH113883 to C.D.S., J.L.L. and B.W.W., and T32 GR0029379 to U.A.T.); Intellectual and Developmental Disabilities Research Center (P50 HD103525 to C.D.S., C.E.R., and J.S.S.; R01 p to D.M.B. and J.L.L.), the March of Dimes Foundation, and institutional support from St. Louis Children’s Hospital, Barnes-Jewish Hospital, and Washington University in St. Louis School of Medicine.

Author contributions

U.A.T. designed the analyses, analyzed data, and wrote the paper. A.L., J.K.K., D.A., and T.S. provided data curation and data analysis. A.N.N. and L.G. assisted with discussions of interpretation and analysis. B.B.W., J.S.S., and J.J.N. assisted with methodology and provided funding. J.L.L., D.M.B., C.E.R. and C.D.S. provided supervision, funding, and edited the manuscript. All authors commented on the manuscript at all stages.

Competing interests

The authors declare no competing interests.

Additional information

Supplementary information The online version contains supplementary material available at <https://doi.org/10.1038/s41467-024-52242-4>.

Correspondence and requests for materials should be addressed to Ursula A. Tooley.

Peer review information *Nature Communications* thanks Wei Gao, Charles Geier, and Alexis Brieant for their contribution to the peer review of this work. A peer review file is available.

Reprints and permissions information is available at <http://www.nature.com/reprints>

Publisher’s note Springer Nature remains neutral with regard to jurisdictional claims in published maps and institutional affiliations.

Open Access This article is licensed under a Creative Commons Attribution-NonCommercial-NoDerivatives 4.0 International License, which permits any non-commercial use, sharing, distribution and reproduction in any medium or format, as long as you give appropriate credit to the original author(s) and the source, provide a link to the Creative Commons licence, and indicate if you modified the licensed material. You do not have permission under this licence to share adapted material derived from this article or parts of it. The images or other third party material in this article are included in the article’s Creative Commons licence, unless indicated otherwise in a credit line to the material. If material is not included in the article’s Creative Commons licence and your intended use is not permitted by statutory regulation or exceeds the permitted use, you will need to obtain permission directly from the copyright holder. To view a copy of this licence, visit <http://creativecommons.org/licenses/by-nc-nd/4.0/>.

© The Author(s) 2024

Acknowledgements

We thank the families involved with the study, and Karen Lukas, Eva Loveless, and Rich Nagel for assistance with scanning neonates. We